FUNDAMENTAL STUDIES OF THE DURABILITY OF MATERIALS FOR INTERCONNECTS IN SOLID OXIDE FUEL CELLS

AGREEMENT NO. DE-FC26-02NT41578
(Start Date September 30, 2002)

J. Hammer, S. Laney, W. Jackson, F. Pettit, & G. Meier
Department of Materials Science & Engineering
University of Pittsburgh

N. Dhanaraj & J. Beuth
Department of Mechanical Engineering
Carnegie Mellon University

SECA Annual Workshop and Core
Technology Program Peer Review

January 28, 2005

University of Pittsburgh

Carnegie Mellon

PROJECT STRUCTURE

NETL

Dr. Lane Wilson — Technical Monitor
Dr. Chris Johnson — NETL Fellowship Mentor

University of Pittsburgh(MSE)

Prof. Frederick. S. Pettit — Co-principal Investigator
Prof. Gerald. H. Meier — Co-principal Investigator

Carnegie Mellon University(ME)

Prof. Jack L. Beuth — Co-principal Investigator

ATI Allegheny Ludlum

Dr. James Rakowski

West Virginia University(ME)

Prof. Bruce Kang

Students

University of Pittsburgh

- Ms. Julie Hammer Graduate Student
- Mr. Wesley Jackson Graduate Student
- Mr. Scot Laney NETL Partnership Fellow

Carnegie Mellon University

- Ms. Nandhini Dhanaraj Graduate Student

Completed

- Ms. Mary Birch B. S. Materials Science
- Ms. Kelly Coyne B.S. Engineering Phys.
- Ms. Carrie Davis B. S. Materials Science
- Mr. Wesley Jackson B. S. Materials Science

Diagram Relating 3 Interconnect Failure Mechanisms

- Three Mechanisms: Scale Thickening, Spallation, Evaporation
  - *Relate Mass Change to an Estimated ASR: Mass Changes in the Pink Region have Excessive ASR due to Thick Chromia Scale*
  - *Use Fracture Mechanics to Get G_c for No Debonding at this Limit: Compare this Value to G_c Measured by Fracture Testing*
  - *For no Debonding, Difference Between Est. Parabolic Growth Curve and Measured Curve (Yellow Region) Quantifies Amount of Scale Evaporation*

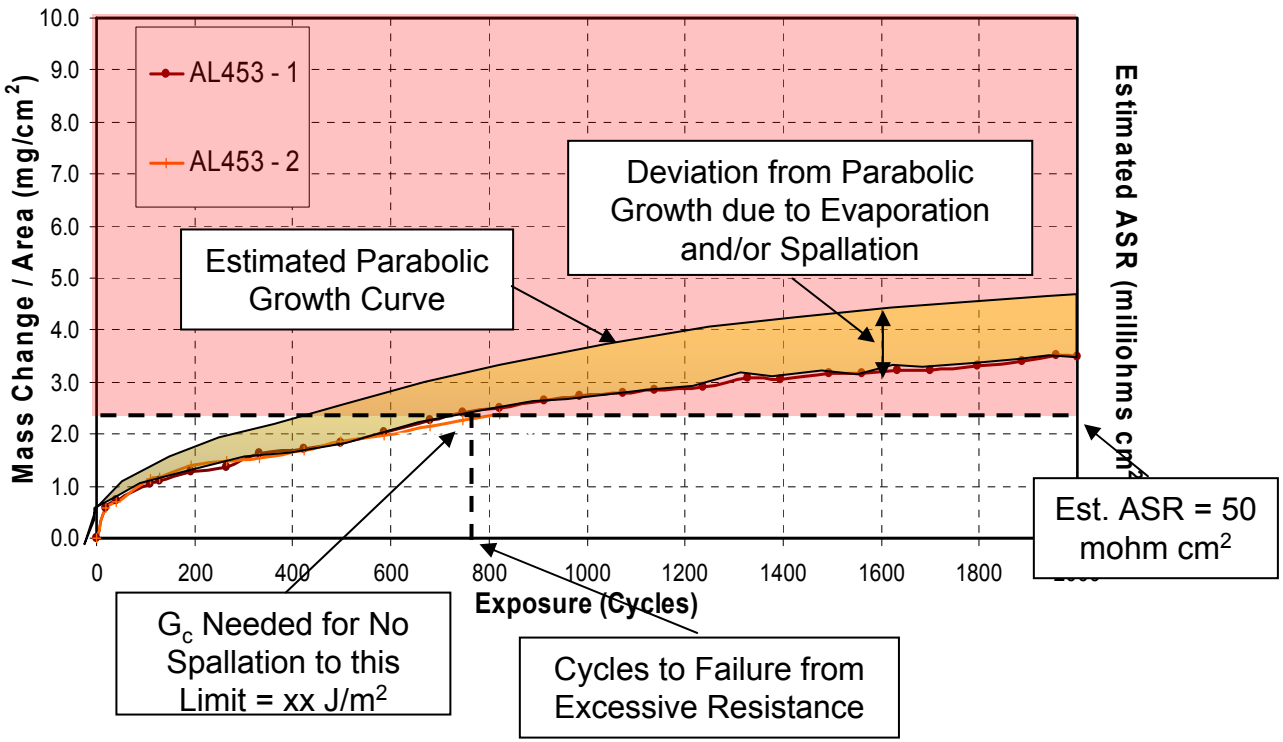

PROGRAM FOCUS
TASK I: Mechanism-Based Evaluation Procedures (Chromia-Forming Alloys)

- Growth Rates of Chromia Scales on Cr and Ferritic Alloys
- Adhesion of Chromia Scales
- Oxide Evaporation
- Complex Atmosphere Testing

*Note: An important theme which cuts across Tasks I and II is the establishment of **accelerated testing protocols**.*

PROGRAM FOCUS;
TASK II: FUNDAMENTAL ASPECTS OF THERMOMECHANICAL BEHAVIOR

- XRD Stress Measurements (Chromia Films)
- Indentation Testing of Interface Adhesion
- Indentation Test Fracture Mechanics Analysis

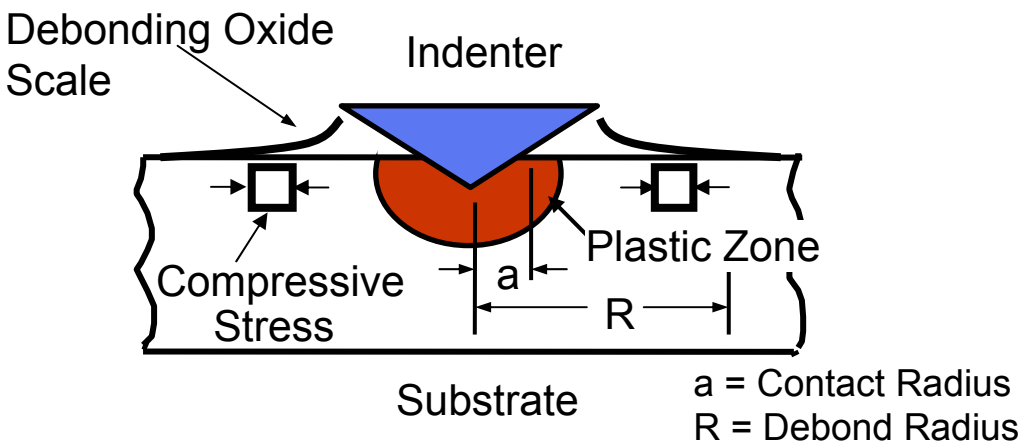

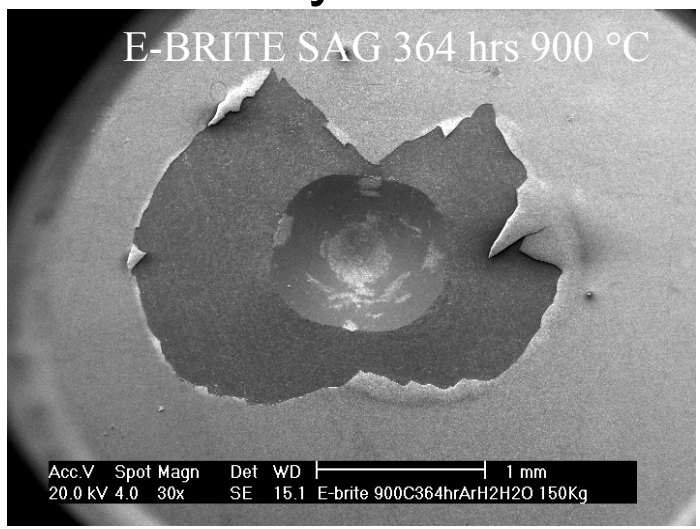

Note: An important theme which cuts across Tasks I and II is the establishment of ***accelerated testing protocols****.*

PROGRAM FOCUS
TASK III: Alternative Material Choices

This Task involves theoretical analysis of possible alternative metallic interconnect schemes including:

- Ni and dispersion-strengthened Ni
- Low CTE Alloys Based on Fe-Ni (Invar)
- Coatings to Suppress Evaporation
- Incorporation of High Conductivity Paths (e.g. Ag)

The most promising systems are being evaluated experimentally with regard to durability and oxide conductivity

Alloy Compositions

Alloy	Fe	Cr	C	Mn	Si	Ni	Mo	Ti	Al	Zr	P	S	La+Ce
Crofer	bal.	22.0	0.005	0.50	---	---	---	0.08	---	---	0.016	0.002	0.06 La
E-brite	bal.	26.0	0.001	0.01	0.025	---	1.0	---	---	---	0.020	0.020	---
26Cr Ferritic	bal.	26.0	---	~ 1.0	~ 1.0	---	1.0	---	---	---	---	---	---
AL453	bal.	22.0	0.030	0.30	0.300	---	---	0.02	0.60	---	0.020	0.030	0.10
ZMG232	bal.	22.0	0.020	0.50	0.400	0.26	---	---	0.21	0.22	---	---	0.04 La

Exposure Conditions

T = 700°C, 800°C, 900°C

One-Hour Cycles

Atmospheres

Dry Air (SCG)

Air + 0.1 atm H_2O

$Ar/H_2/H_2O$ (SAG)

(p_{O2} = 10^{-20} atm at 700°C and 10^{-17} atm at 900°C)

Previous Results

- Oxidation in wet air produced the most severe degradation at 900˚C (accelerated chromia growth on Crofer and AL453 and increased spallation from 26 Cr Ferritic).
- ASR correlated with oxide thickness.
- Thin specimens deform under oxidation-induced stresses.
- Sigma phase formed in 26 Cr Ferritic at 700^{o}C.

Focus of Presentation

- Purity in Ferritic Alloys
- Chromia Volatilization Problem

Effects of Alloy Purity

Oxidation, ASR, and Metallurgical Stability are all influenced by minor impurities.

Simulated Anode Gas (Ar-4%H_2, H_2O) Exposures – 700°C

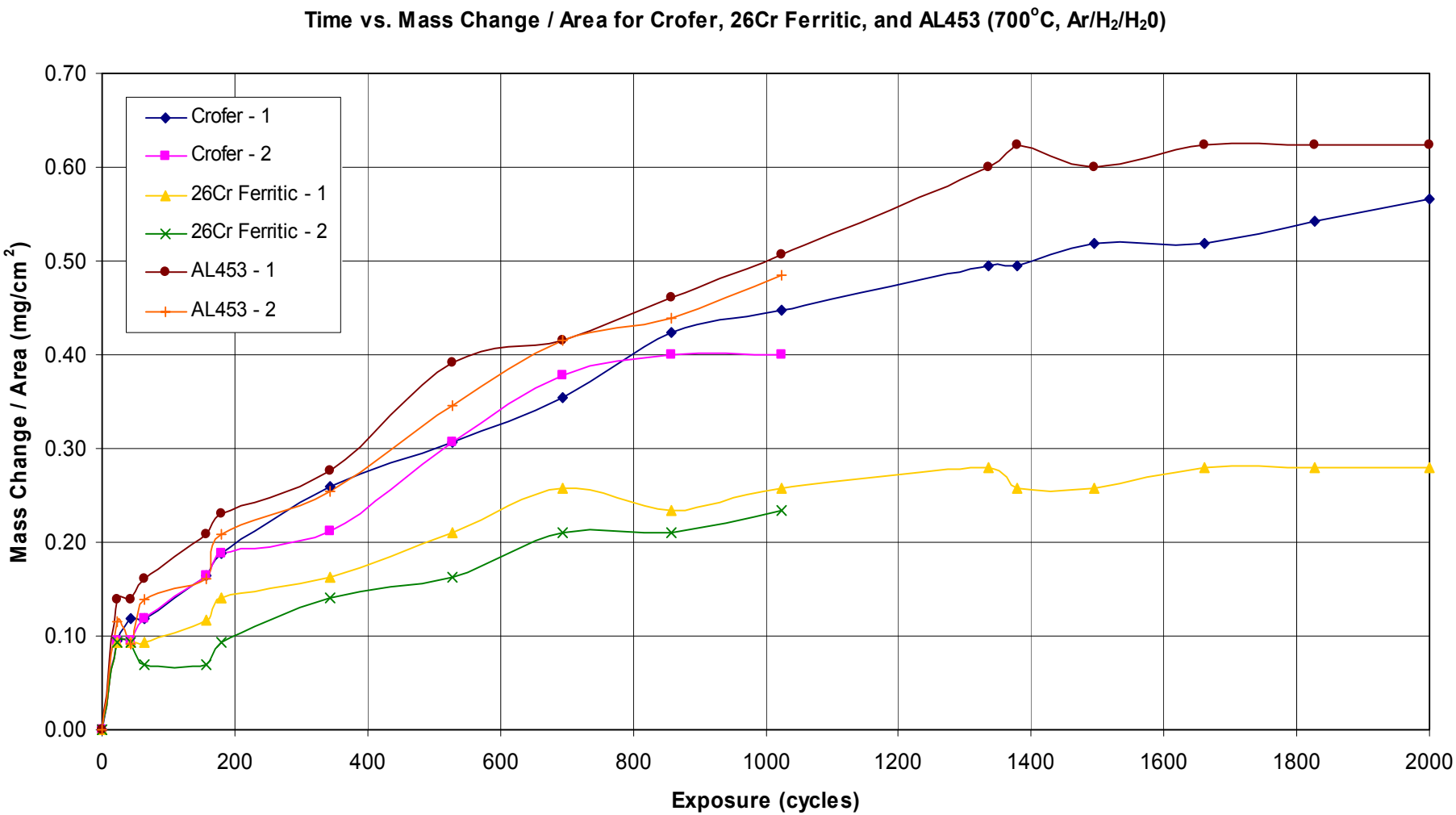

Simulated Anode Gas (Ar-4%H_2, H_2O) Exposures – 700°C

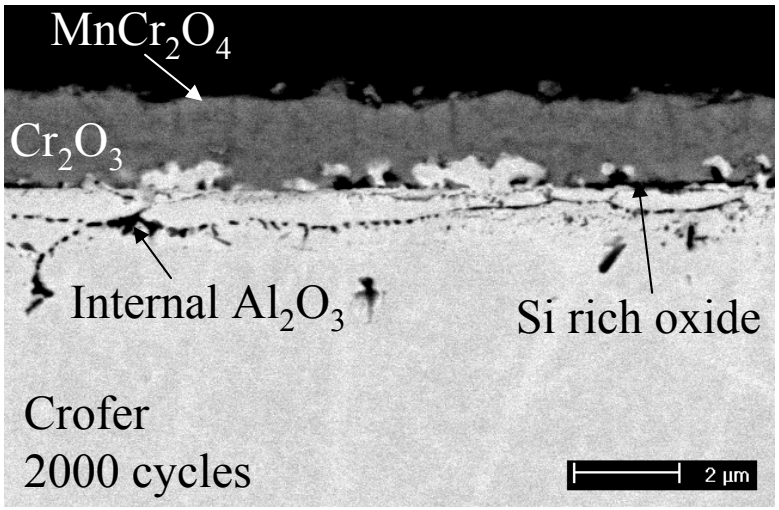

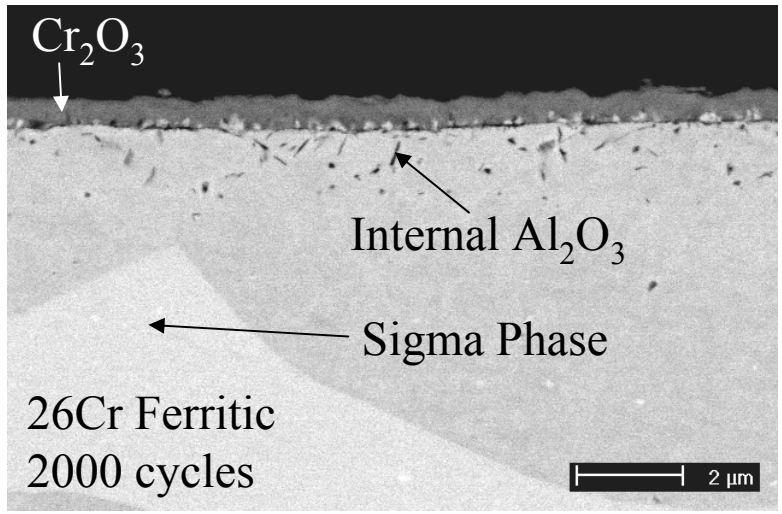

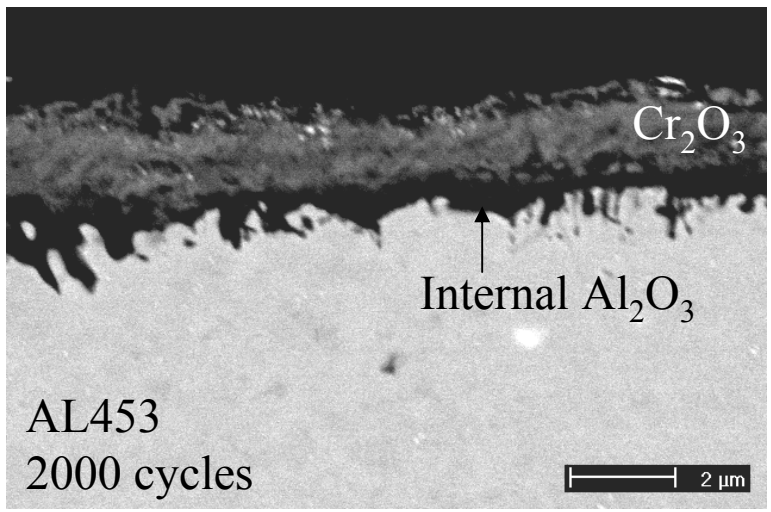

Sigma Phase in 26Cr Ferritic at 700°C

Current experiments show σ in 26Cr Ferritic after 300 h, none in E-BRITE

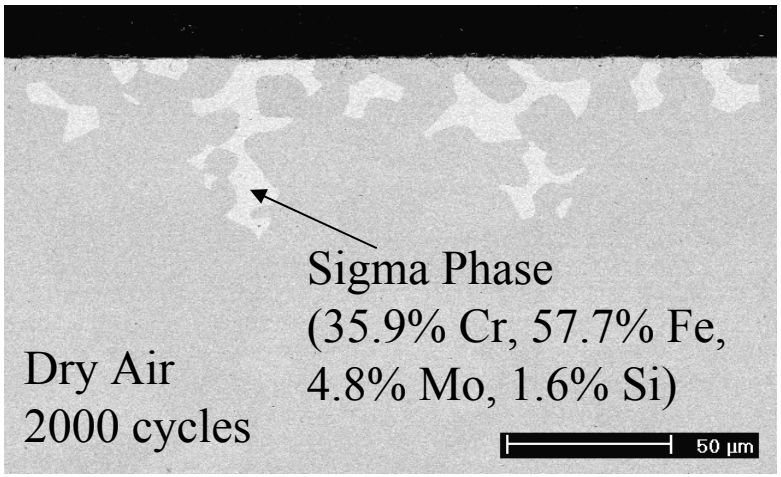

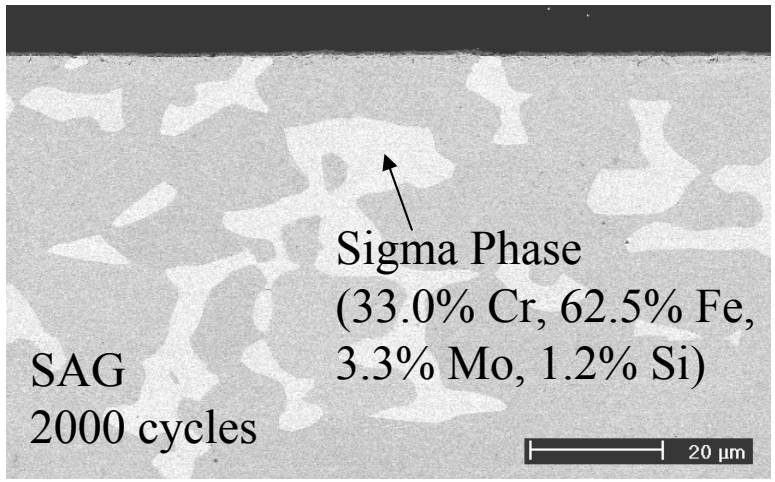

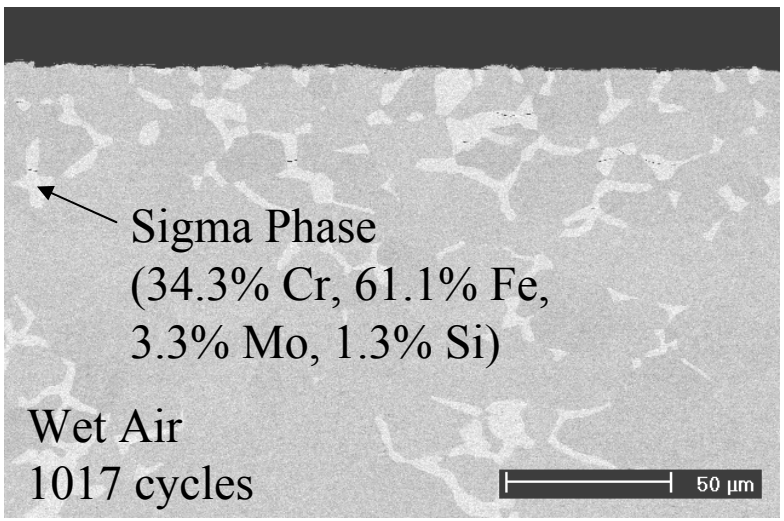

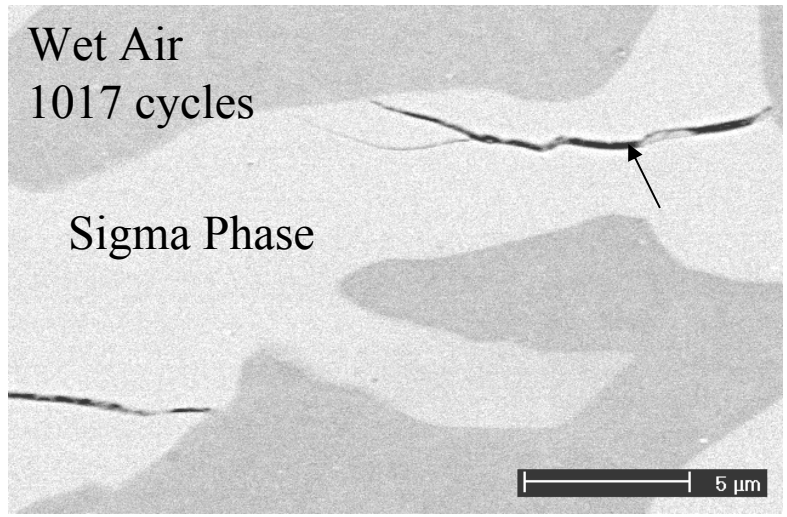

Wet Air (0.1 atm H_2O) Exposures – 800°C (JS-3, old Crofer, new Crofer)

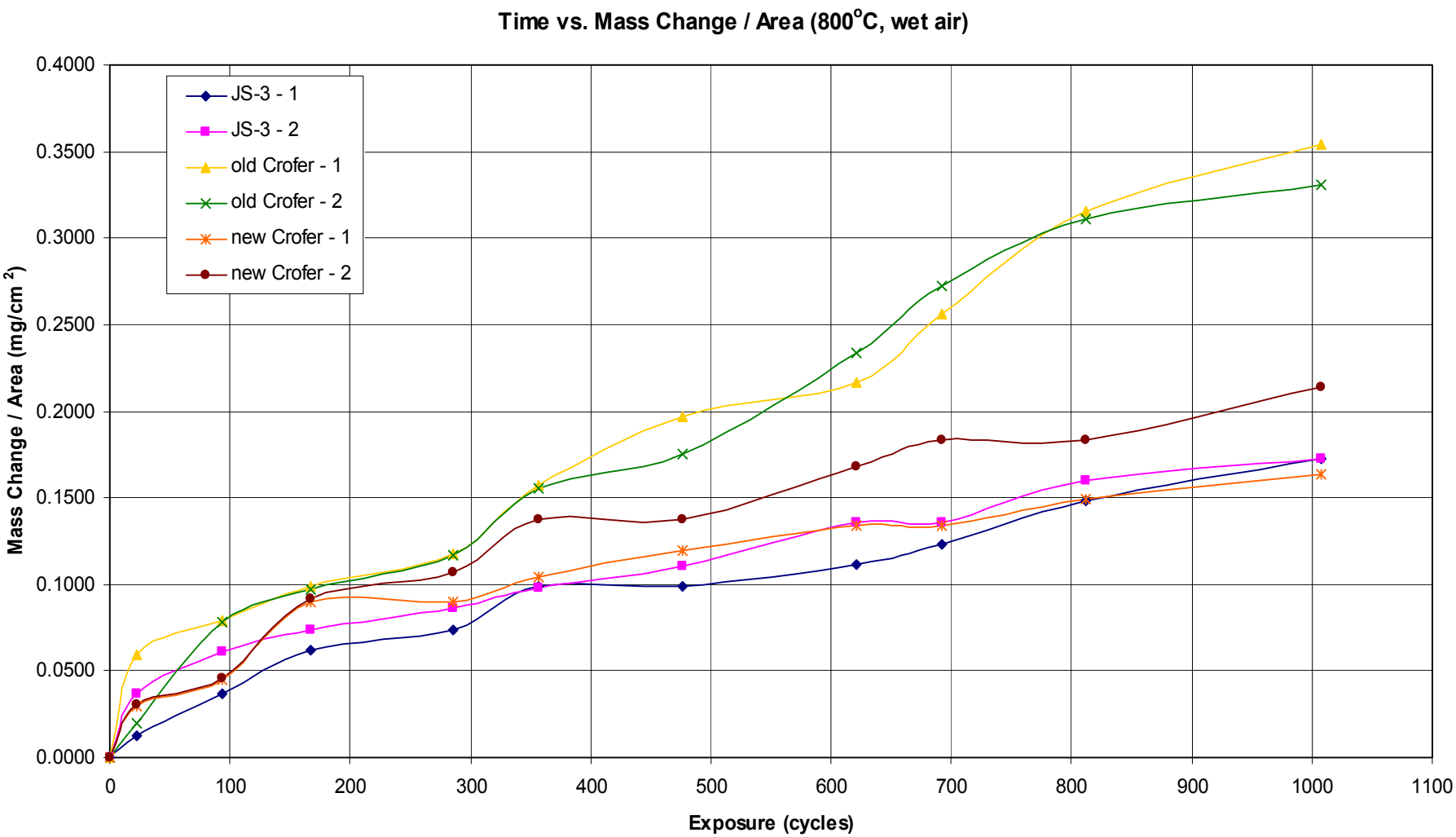

Wet Air (0.1 atm H_2O) Exposures – 800°C (JS-3, old Crofer, new Crofer)

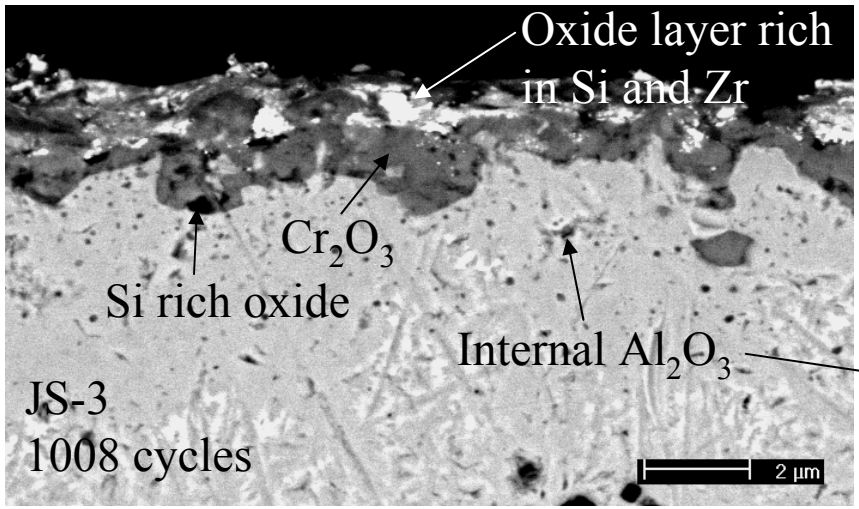

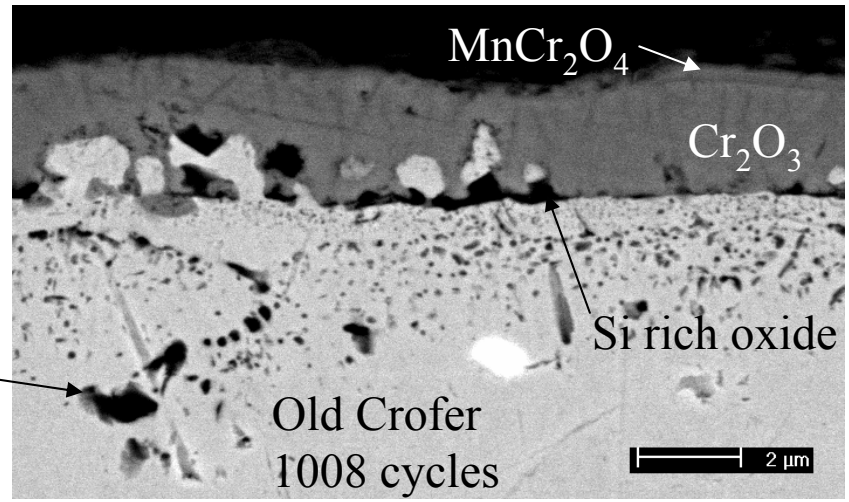

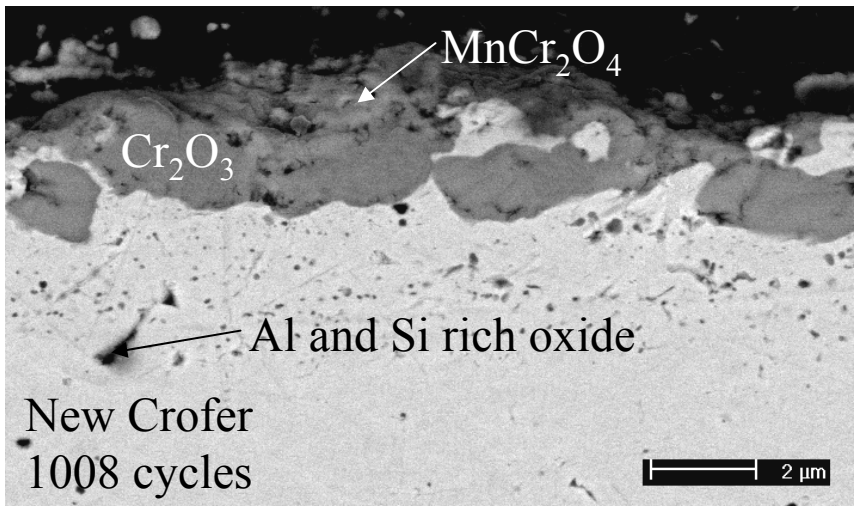

Solutions to the Evaporation Problem

- Overgrowth of Low-Volatility Oxide
- Use of Coatings
- Development of Cr-free Interconnects.

Oxide Electrical Properties

Oxide	ρ (ohm cm) in air
SiO_2	7×10^6 (600°C)
Al_2O_3	5×10^8 (700°C)
Cr_2O_3	1×10^2 (800°C)
NiO	5 (900°C)
CoO	1 (950°C)
TiO_2*	3×10^2 (1000°C)

* Note: $\rho_{TiO2} = 5 \times 10^{-1}$ ohm cm at $p_{O2} = 10^{-16}$ atm

Chromia Evaporation

Crofer

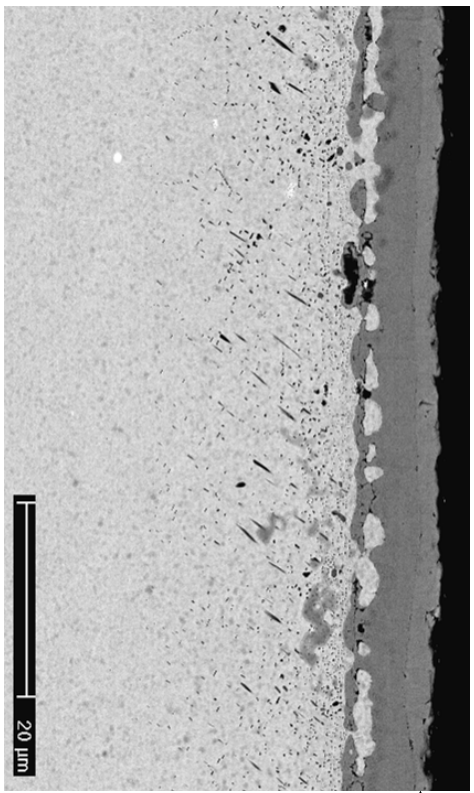

$MnCr_2O_4$

$$Cr_2O_3(s) + \tfrac{3}{2}O_2(g) = 2CrO_3(g)$$

$$p_{CrO_3} = K^{\frac{1}{2}} a_{cr_2O_3}^{\frac{1}{2}} p_{O_2}^{\frac{3}{4}}$$

$$MnO(s) + Cr_2O_3(s) = MnCr_2O_4(s)$$

$$\Delta G^o_{1100K} \approx -89 KJ/mole$$

Chromia Saturation $a_{Cr_2O_3} = 1$ $p_{CrO_3} = 4x10^{-11} atm$

MnO Saturation

$a_{Cr_2O_3} = 6x10^{-5}$ $p_{CrO_3} = 3x10^{-13} atm$

$LaCrO_3$ (Activity data from Hilpert et al)

$a_{Cr_2O_3} = 10^{-7}$ $p_{CrO_3} = 1x10^{-14} atm$

Partial pressures of CrO_3 in Equilibrium with Cr_2O_3, MnO-saturated $MnCr_2O_4$, and $LaCrO_3$

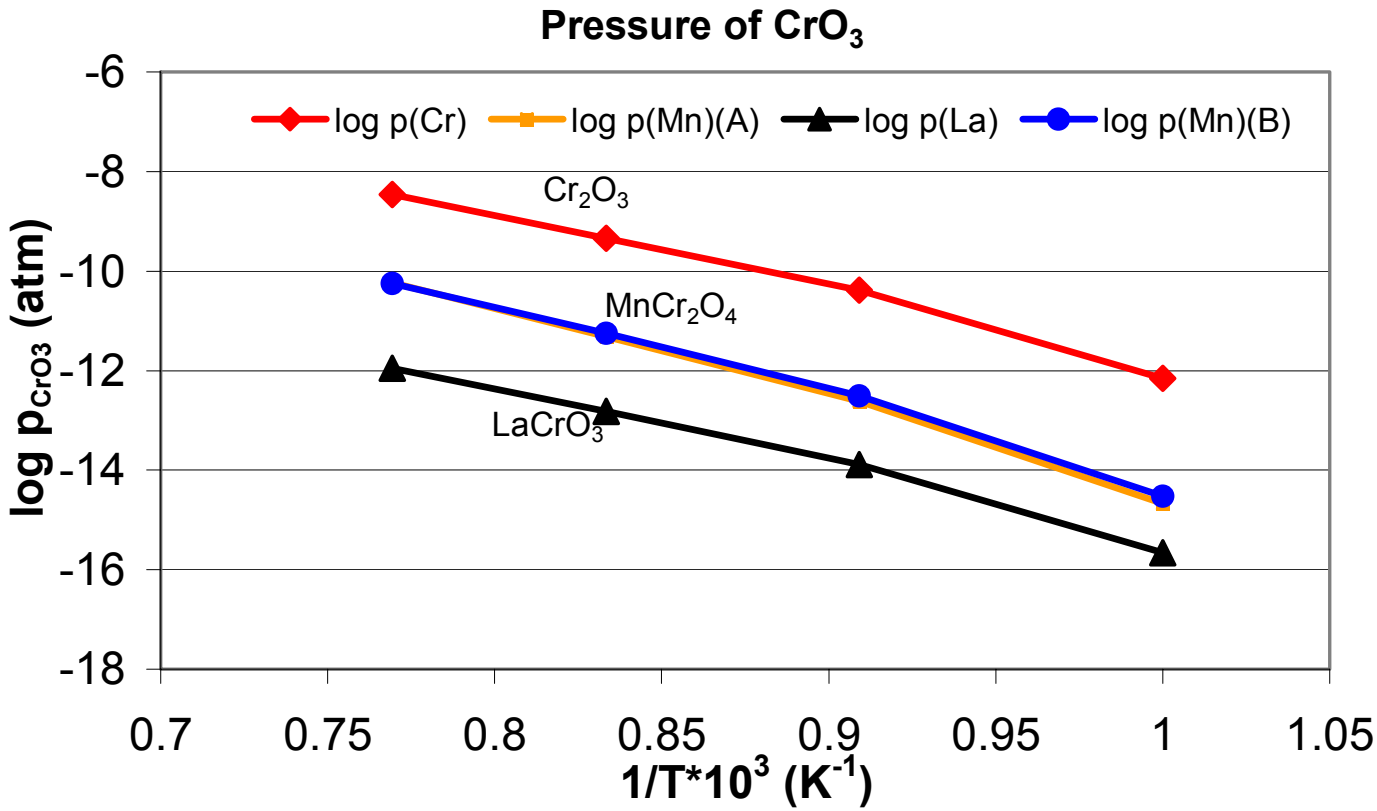

Note: similar reductions would be achieved in the pressure of $CrO_2(OH)_2$

Oxide Evaporation from Ni-Cr Alloys

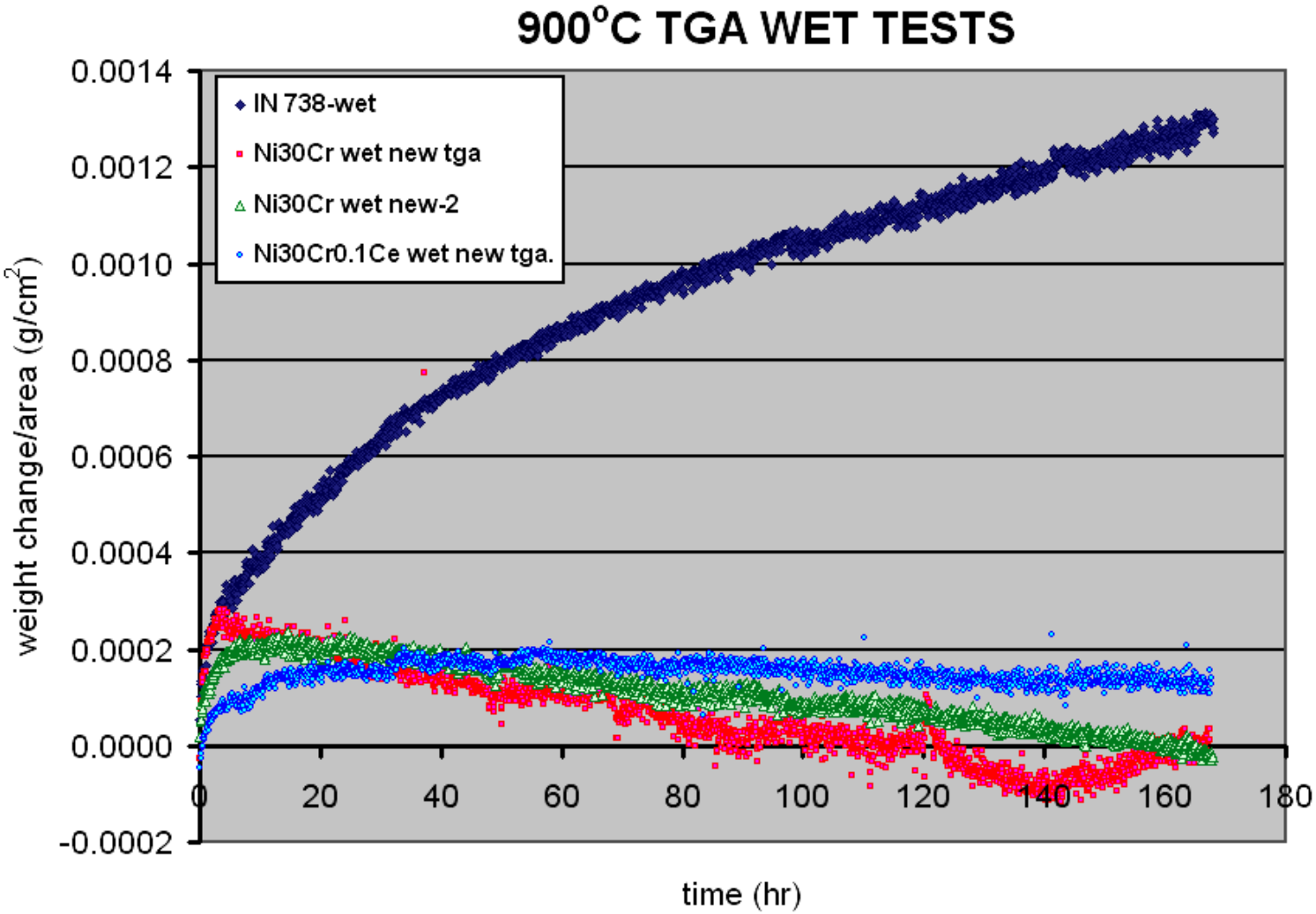

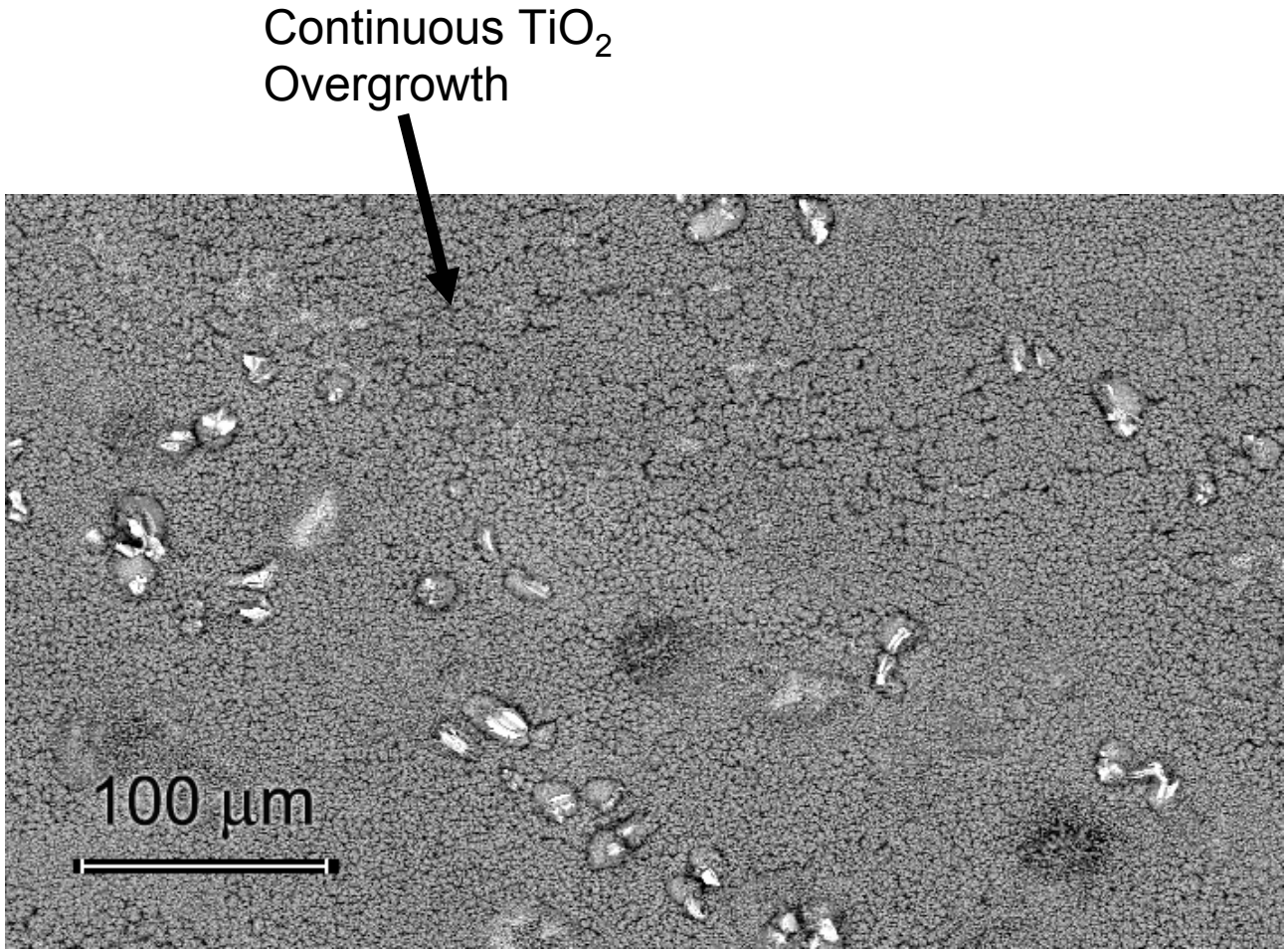

IN 738 at 900°C in wet air (0.1 atm) isothermal-168 hr

Vapor Pressures – 1100 K

Metal	p_M (atm)	p_{O2}-M/MO (atm)	Oxide – p_{Oxide} (atm)
Cr	$7 X10^{-12}$	$1 X 10^{-27}$	CrO_3 - $4 X 10^{-11}$
Fe	$1 X 10^{-12}$	$9 X 10^{-20}$	FeO - $1 X 10^{-16}$
Ni	$2 X 10^{-13}$	$4 X 10^{-14}$	NiO - $1 X 10^{-16}$
Cu	$6 X10^{-10}$	$4 X 10^{-9}$	CuO - $5 X10^{-13}$
Ti	$1 X 10^{-15}$	$4 X 10^{-36}$	TiO_2 - $1 X 10^{-20}$

Collaborative work with Allegheny Ludlum is directed at producing the "TiO_2 Effect" in a ferritic alloy.

Various Thicknesses of $LaCrO_3$ Based Coatings

2hrs Ar-H_2 800°C

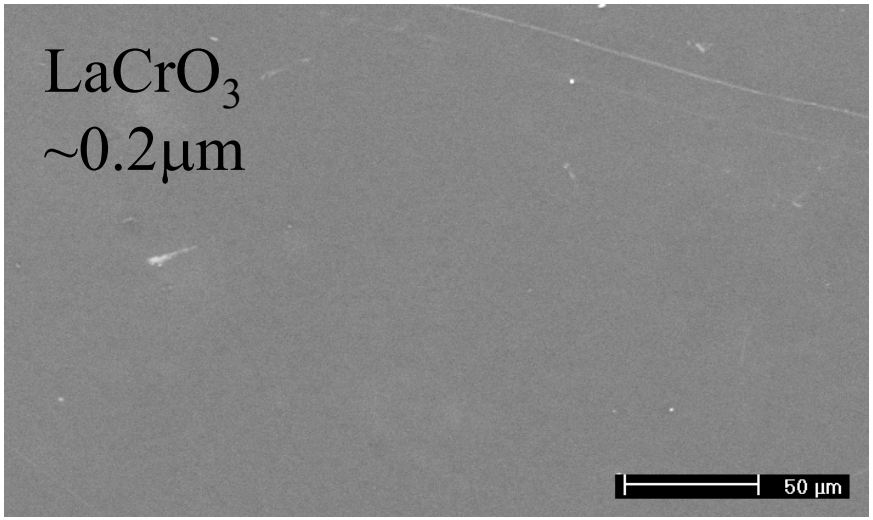

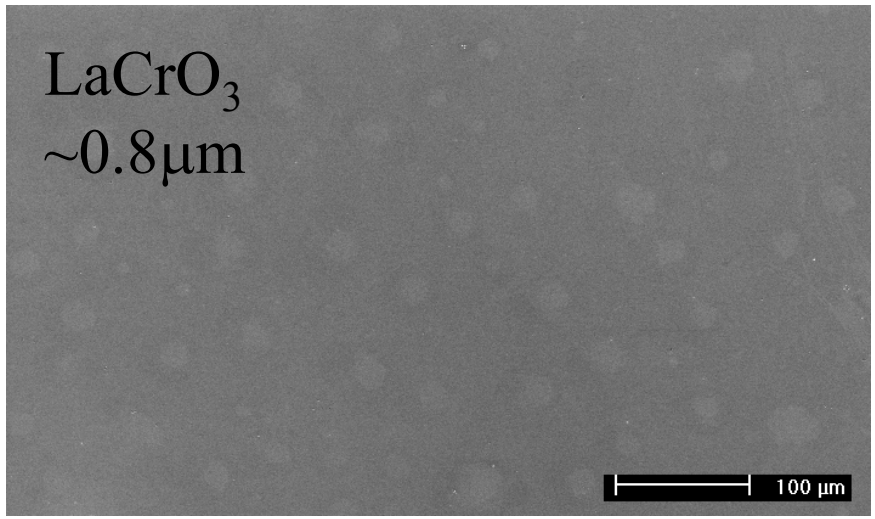

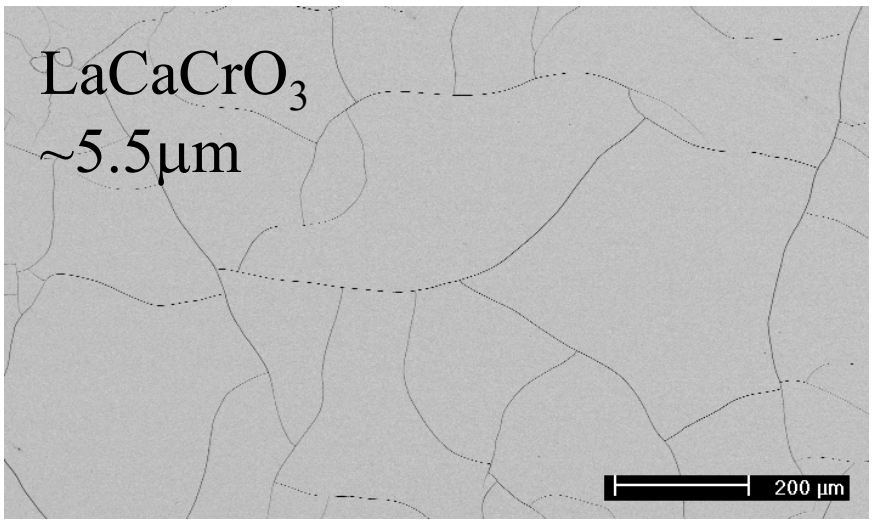

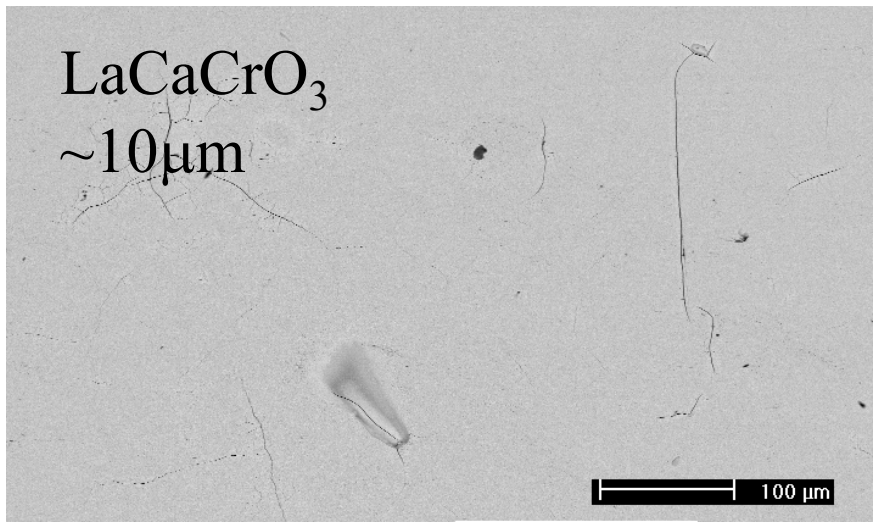

Indentation of Exposed Chromite-Coated Specimens

- $La_{0.8}Sr_{0.2}CrO_3$ on E-BRITE (PNNL) and $LaCrO_3$ on SS 446 (Drexel/NETL) *Exposed in Dry Air, 100 Hrs, 900°C*
- Debonding More Extensive for $La_{0.8}Sr_{0.2}CrO_3$ and Now Occurs for $LaCrO_3$
- Chromia Scale has Formed Under Both Coatings, Debonding at Chromia/Metal Interface
- Coatings Seem to Reduce Scale Growth Rate But Increase Debonding;

As Processed:

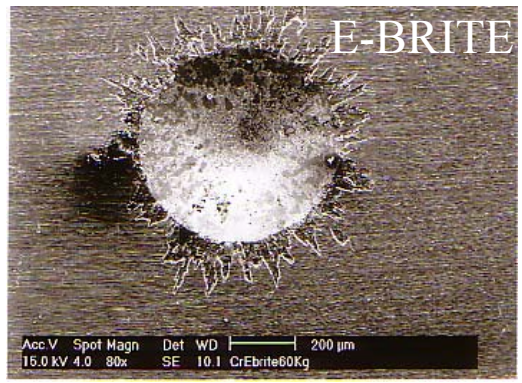

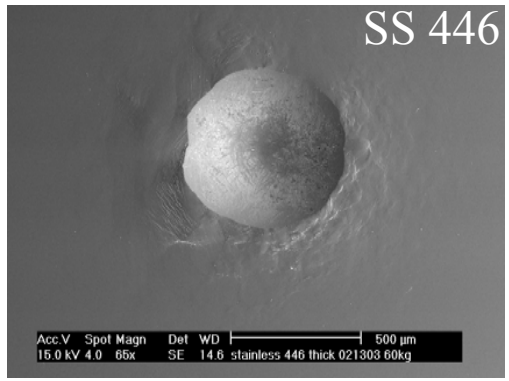

Exposed 100hr 900°C:

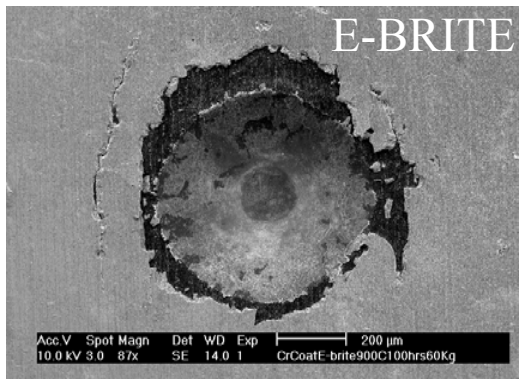

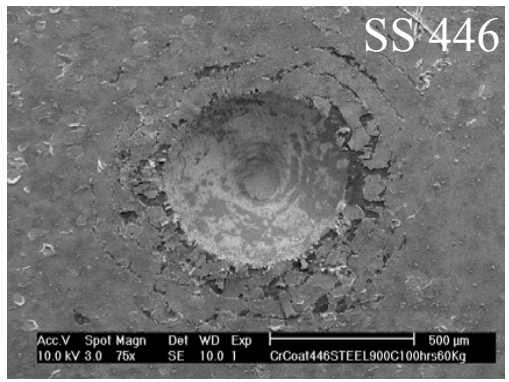

Behavior of nickel in a fuel cell environment?

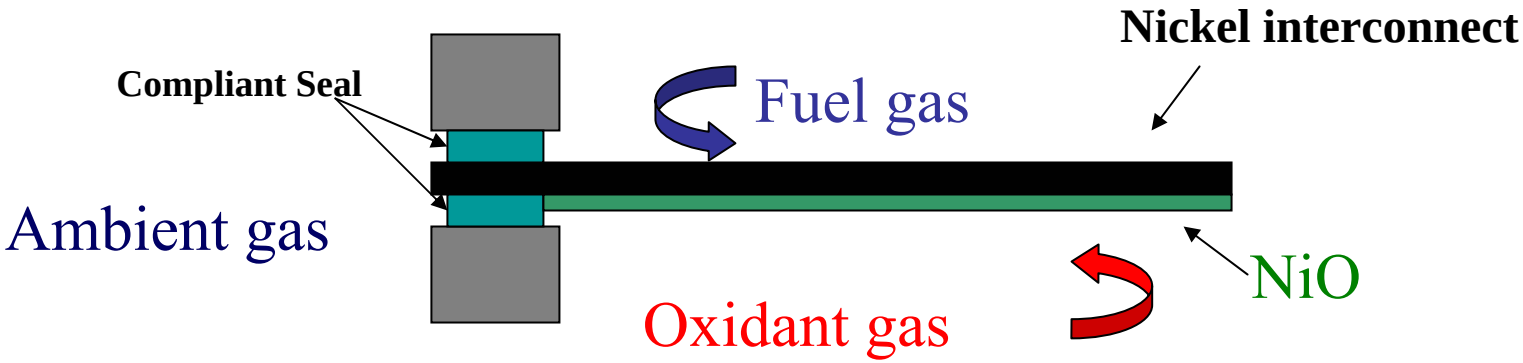

- NiO will form on cathode side, not anode side

Comparison of Ni with Chromia forming alloys

- NiO evaporation is extremely low
- NiO grows faster
- Conductivity dominated by defects
- Conductivity is p_{O_2} dependent

- Contamination from CrO_3 evaporation has produced deleterious effects
- The conductivity of Cr_2O_3 does not have a strong dependence on p_{O_2}

Improving the properties of nickel in a fuel cell environment

- Reduce growth rate
  - Coating with reactive element, e.g. Sr, Ce, La (NiO g.b.s)
  - Alloying, e.g. Cu (lattice transport by Ni vacancies)
- Increase conductivity
  - Doping the scale, e.g. Cu (increase $h^{\bullet}$ conc.)
- High Conductivity via
  - Ni mesh/silver system
  - Silver studs

TGA 800°C

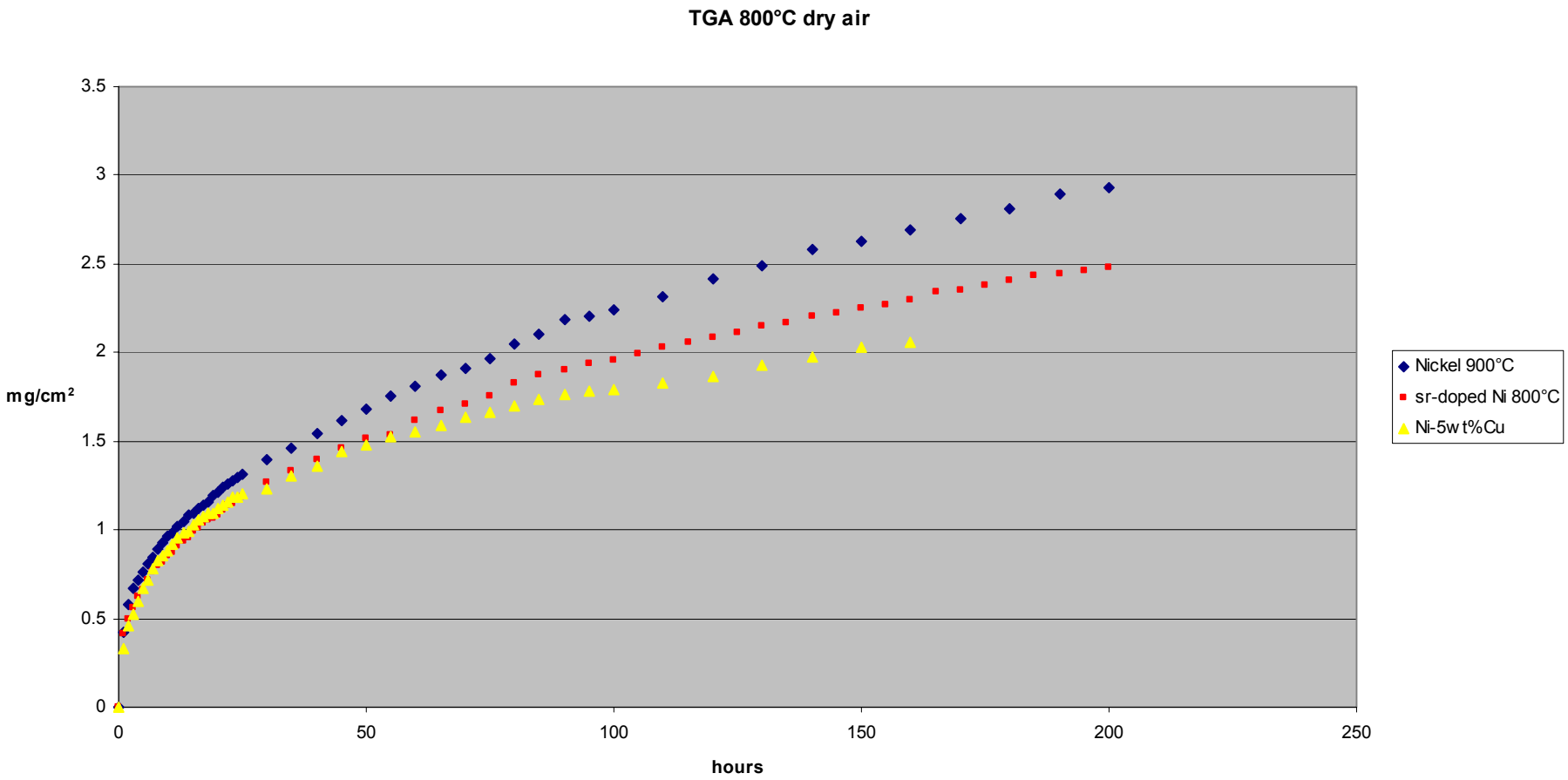
TGA 800°C dry air
mg/cm²
hours
0
0.5
1
1.5
2
2.5
3
3.5
0
50
100
150
200
250
Nickel 900°C
sr-doped Ni 800°C
Ni-5wt%Cu

Dual Atmosphere Apparatus

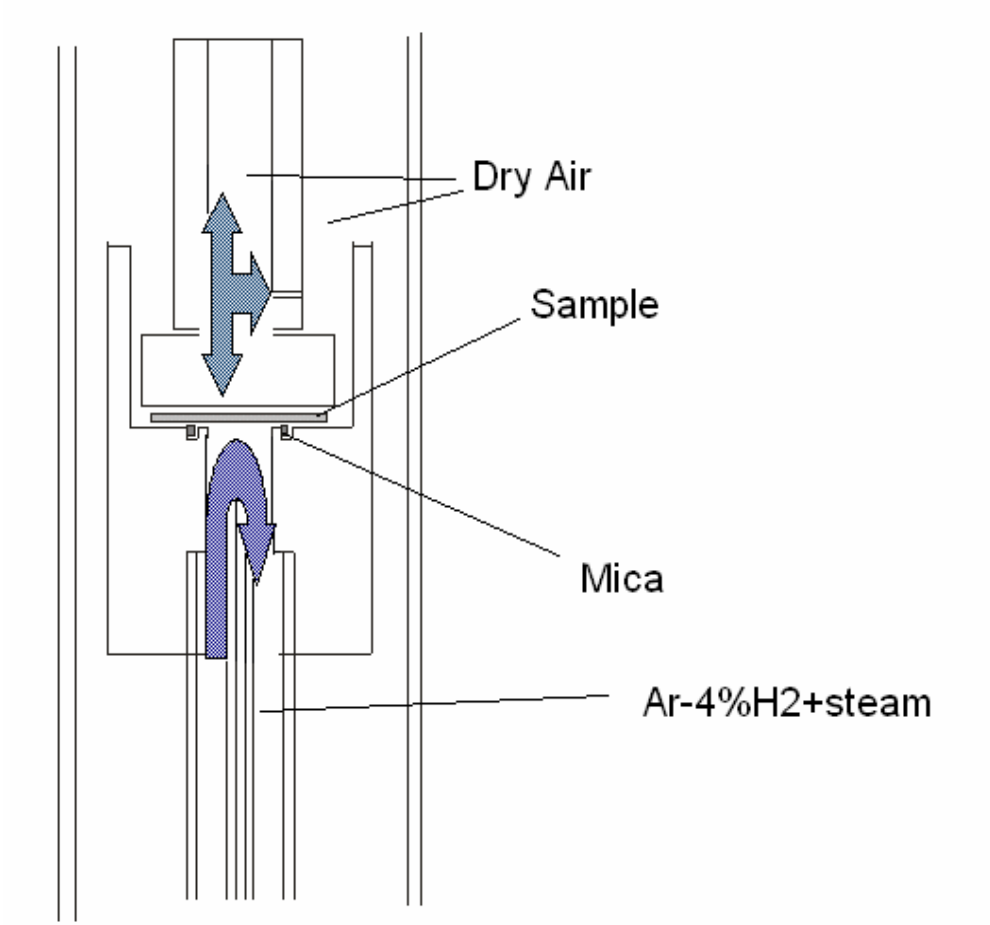

Results-E-Brite-Dry Air

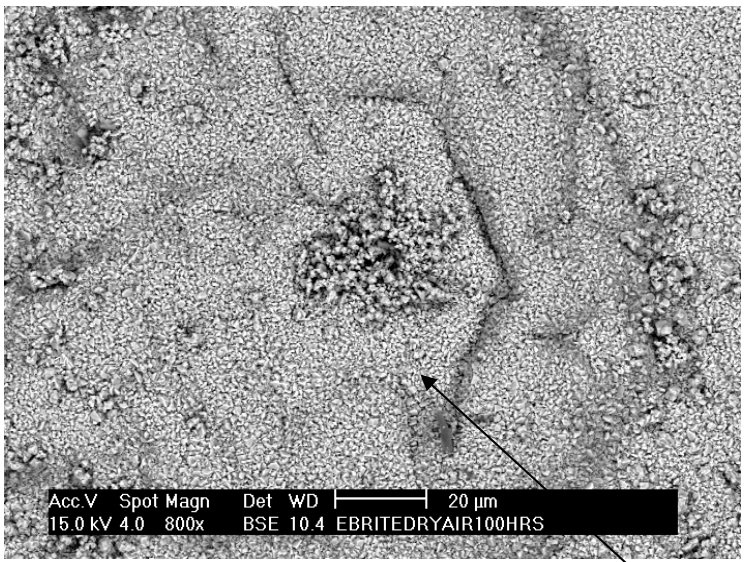

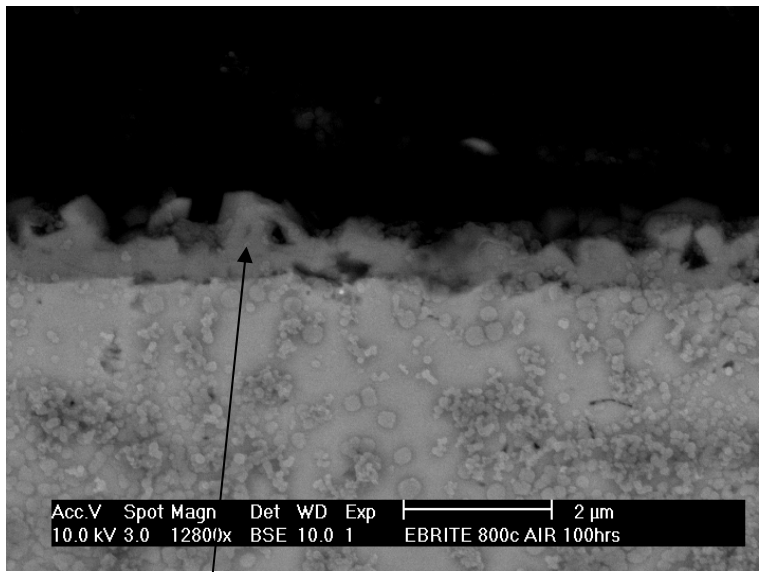

Chromia- .5µm

Results-E-Brite Dual Atmosphere Apparatus- Air side

Iron oxide nodules 7µm

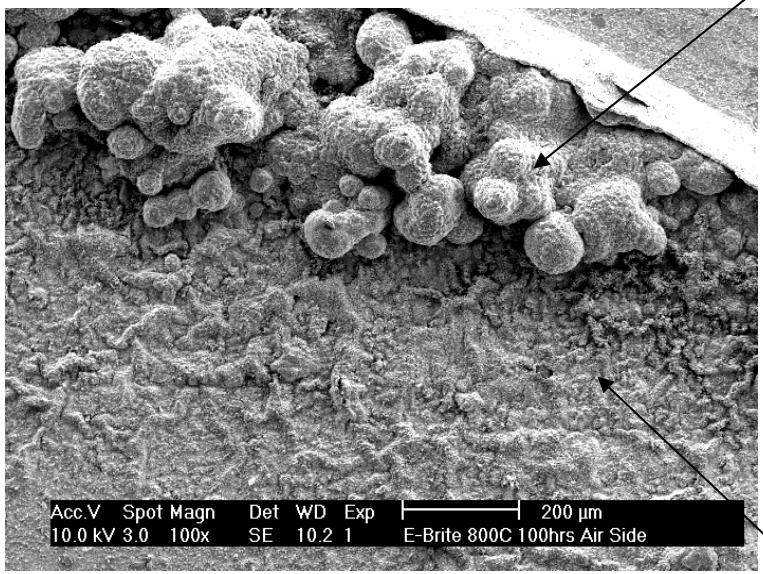

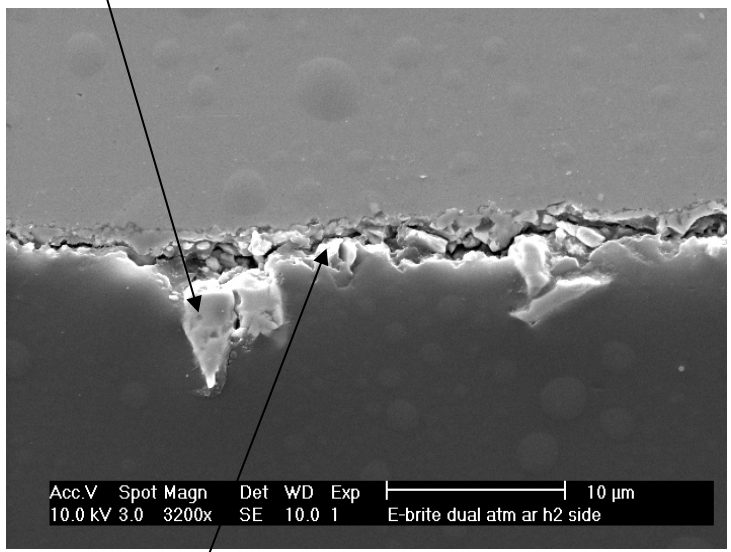

Chromia- 1.5µm

Dual Atmosphere Experimental Apparatus

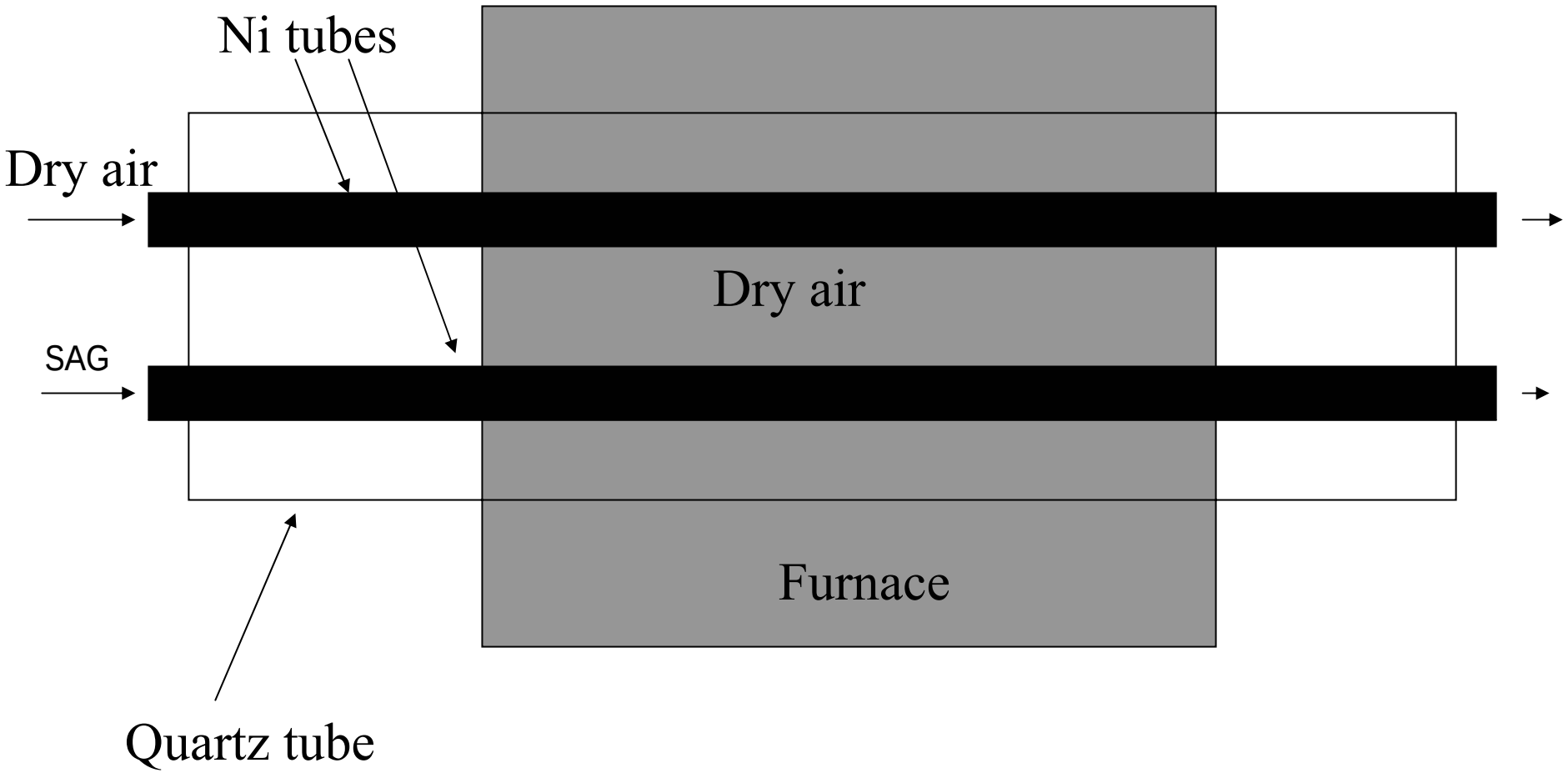

600 hours 800°C

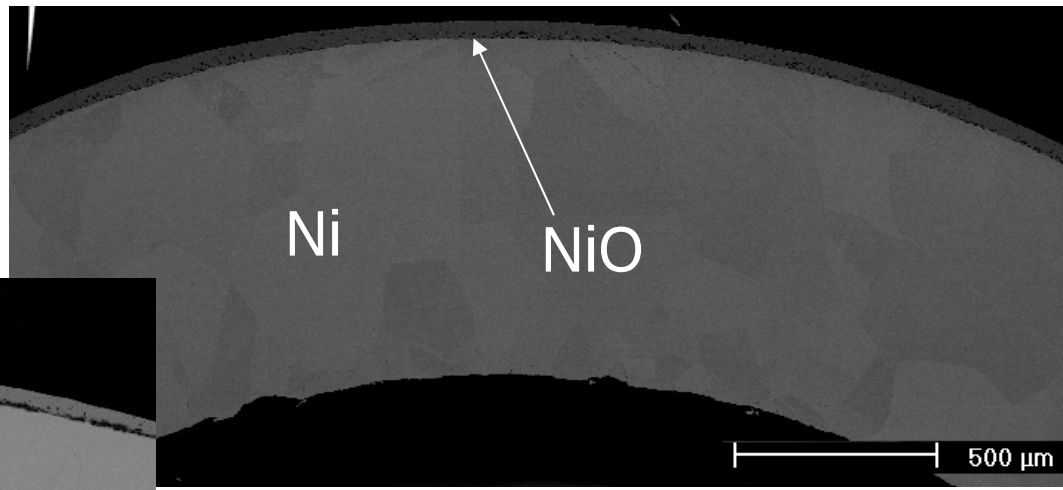

Ar-10%$H_2$0-4%H_2/Air

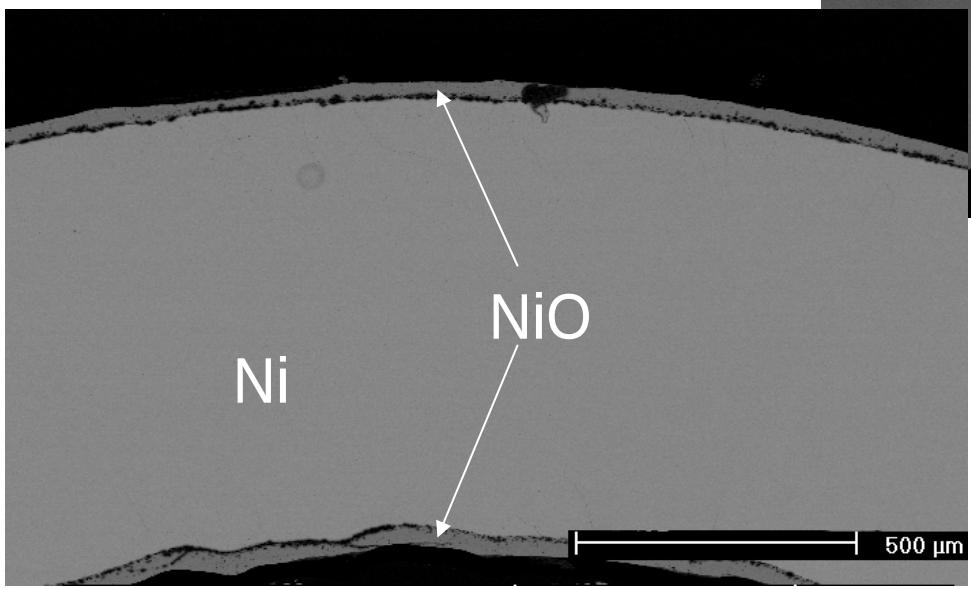

Air/Air

400 Hours 800°C

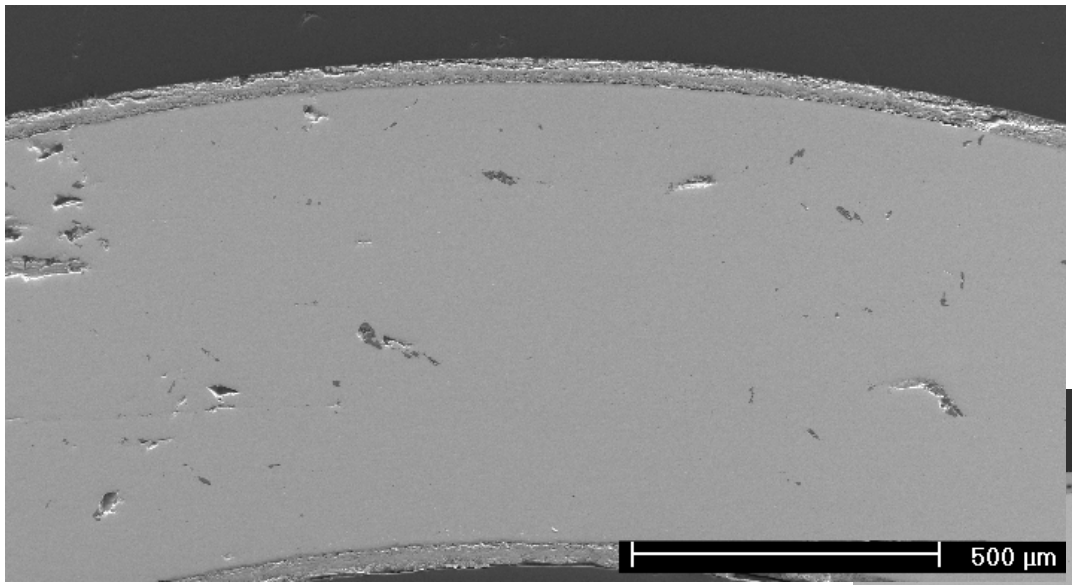

Air/Air

Ar-4%H_2/Air

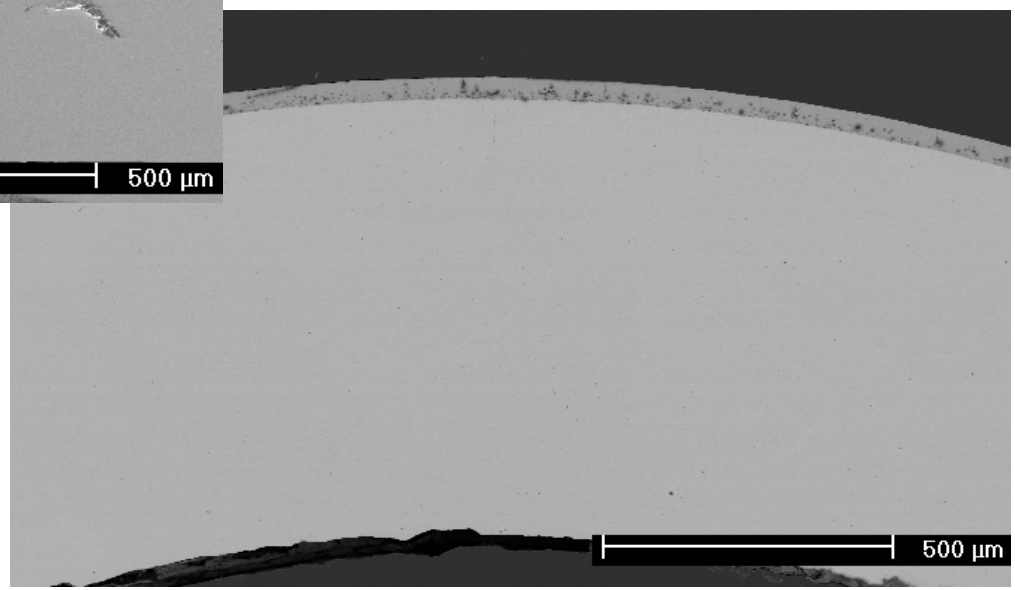

600 Hours 800°C

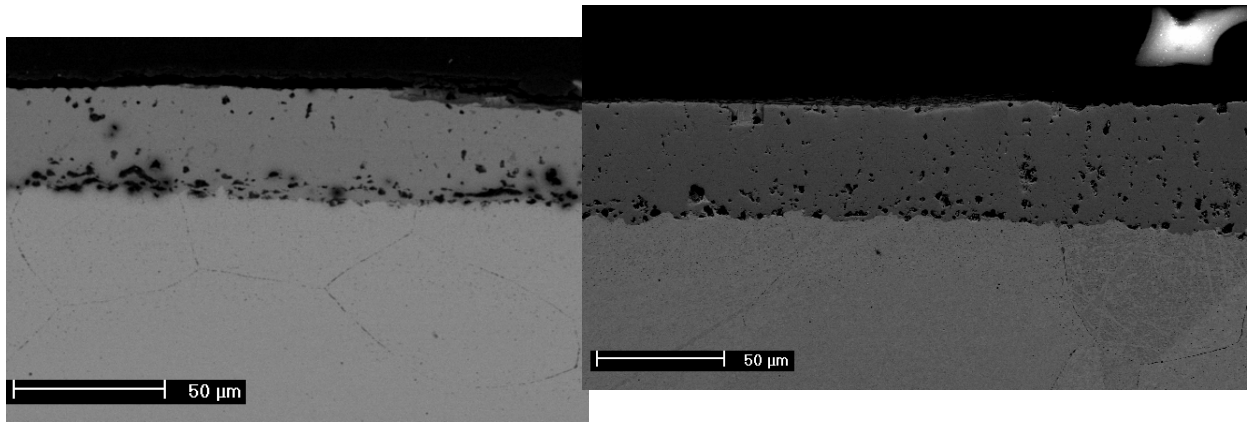

Air/Air

Ar-10%$H_2$0-4%H_2/Air

400 Hours 800°C

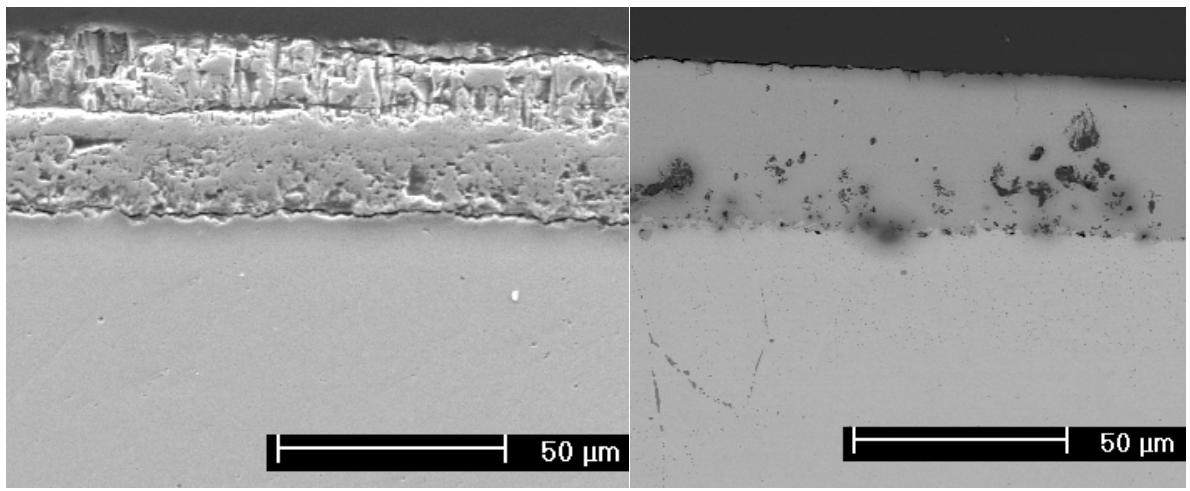

Ar-4 % H_2

Oxygen and Hydrogen Concentration Profiles

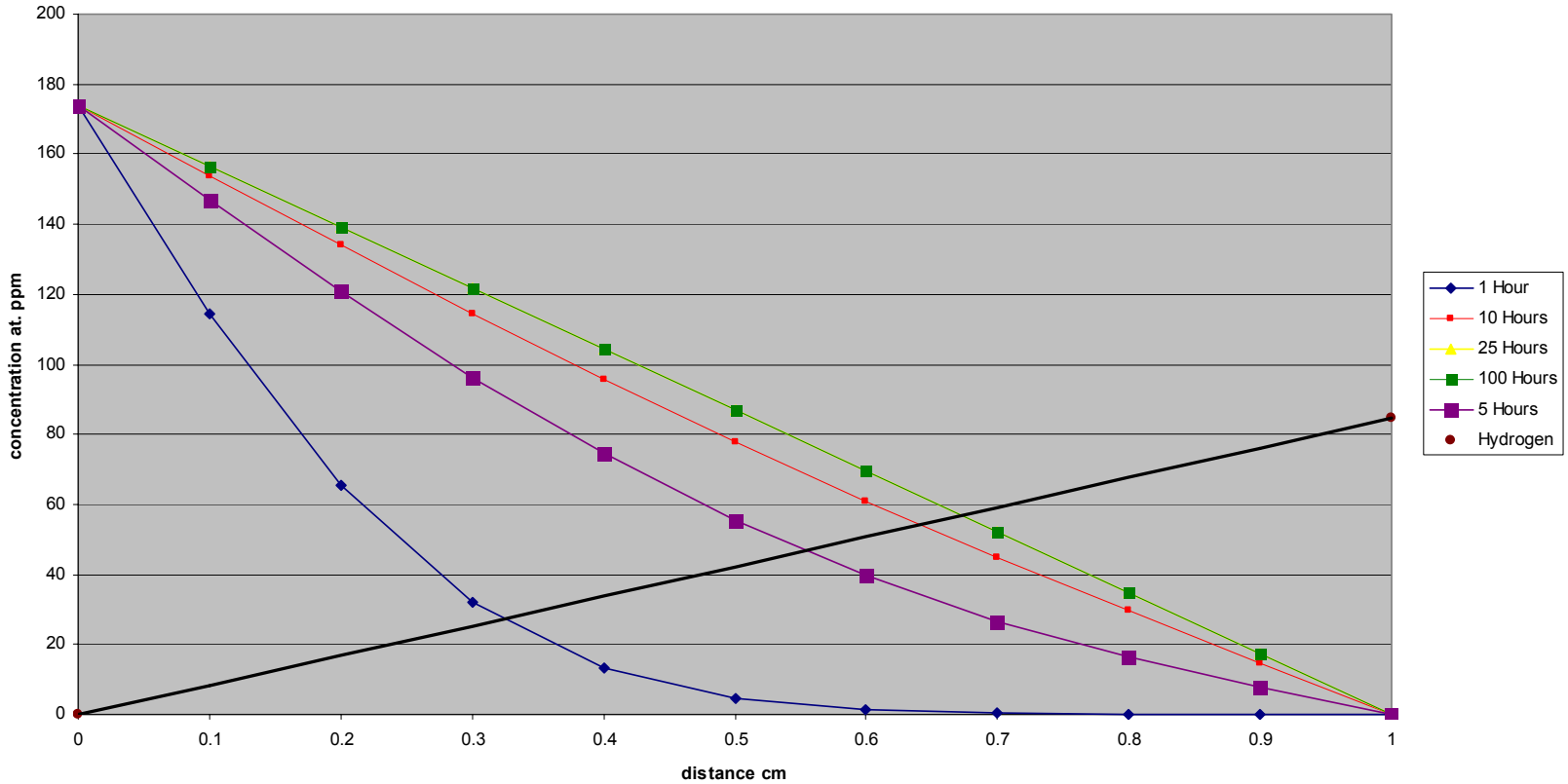

Future Work

- Ferritic Alloys (collaboration with A-L)

  Prepare high-purity alloys

  Achieve evaporation suppression with Ti.
- Coatings to Suppress Evaporation

  Crack Sealing

    Al from vapor phase

    Al from liquid phase

    Al_2O_3 and La_2O_3 from liquid precursors (Prof. C. Levi – UCSB)

  Cyclic Thermal Exposures
- Optimizing Ni Interconnects

  Doping

  Alloying

  Use of Ag Conduction Paths

Compositions of Sigma Phase and Ferrite in Affected Zone

Atmosphere	Exposure Time (hrs)	Composition of Sigma Phase				Composition of Ferrite in Affected Zone			
		wt% Fe	wt% Cr	wt% Mo	wt% Si	wt% Fe	wt% Cr	wt% Mo	wt% Si
Dry Air	1019	59.94	35.06	4.00	1.00	74.69	23.41	1.08	0.83
Dry Air	2000	57.71	35.87	4.82	1.61	70.59	26.05	1.95	1.42
Wet Air	1017	61.15	34.25	3.34	1.27	76.07	21.99	0.98	0.97
SAG	1023	60.43	34.79	3.83	0.96	74.54	23.35	1.24	0.88
SAG	2000	62.51	32.97	3.32	1.21	76.25	21.85	0.96	0.94
Average - Dry Air		58.83	35.46	4.41	1.31	72.64	24.73	1.51	1.12
Average - Wet Air		61.15	34.25	3.34	1.27	76.07	21.99	0.98	0.97
Average - SAG		61.47	33.88	3.57	1.08	75.39	22.60	1.10	0.91
Total Average		60.35	34.59	3.86	1.21	74.43	23.33	1.24	1.01

Simulated Anode Gas (Ar-4%H_2, H_2O) Exposures – 900°C

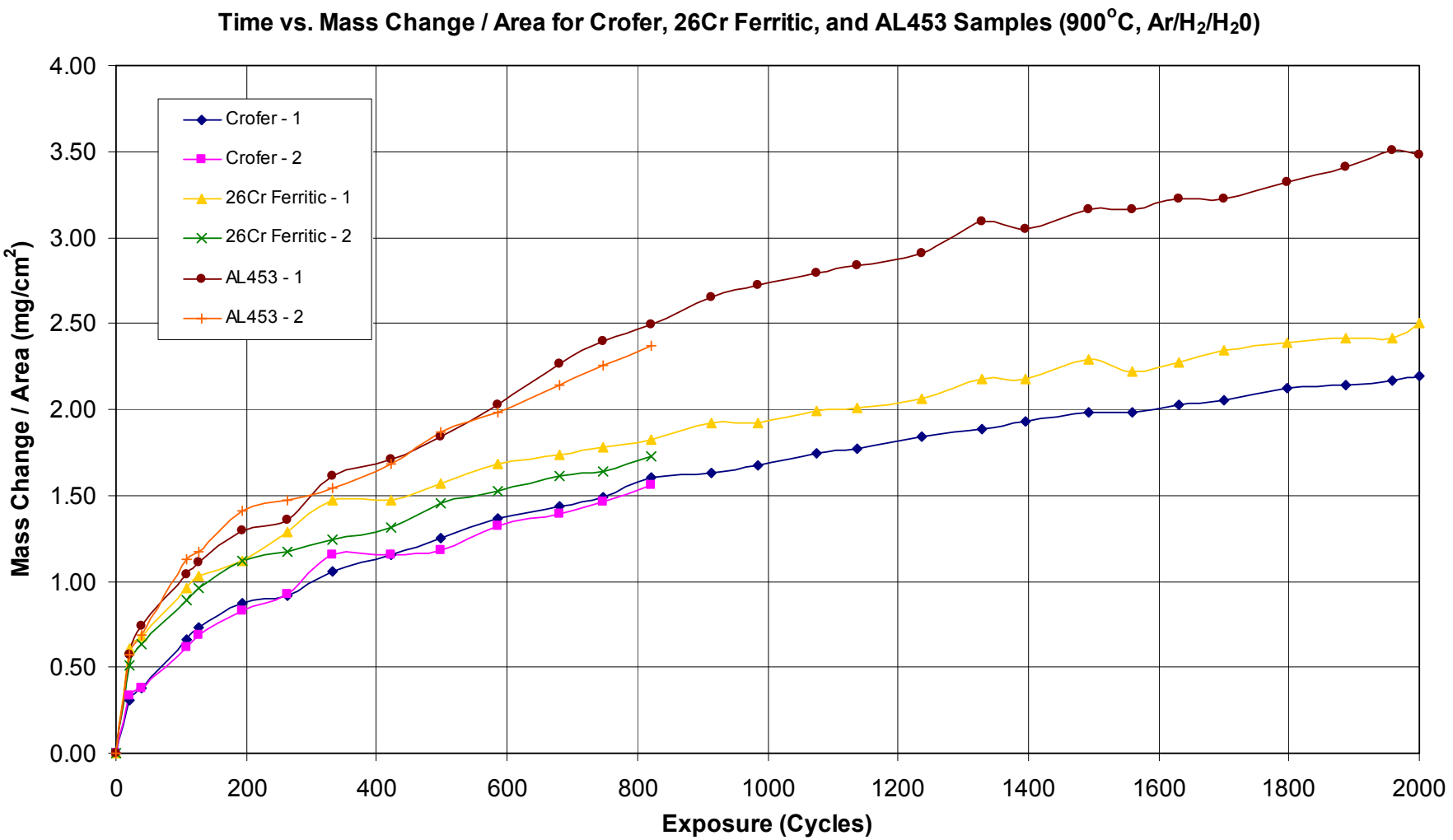

Simulated Anode Gas (Ar-4%H_2, H_2O) Exposures – 900°C

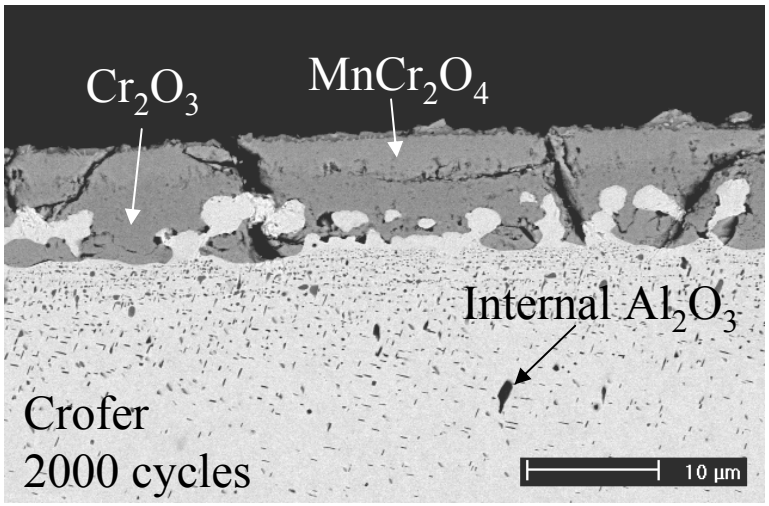

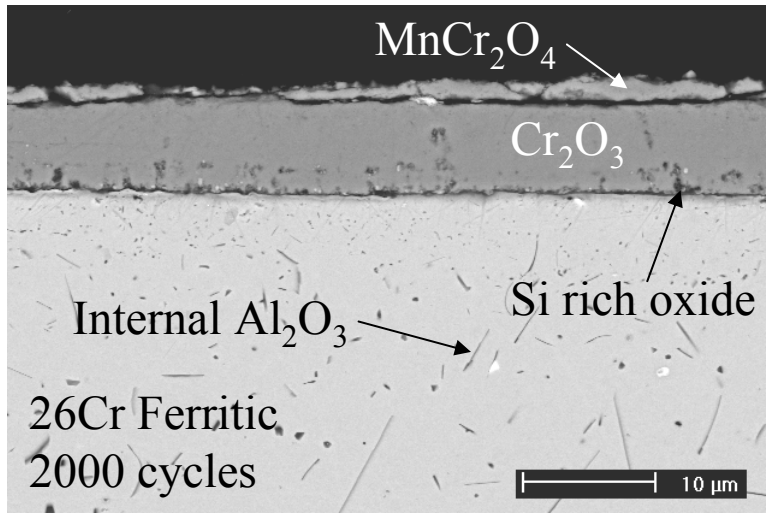

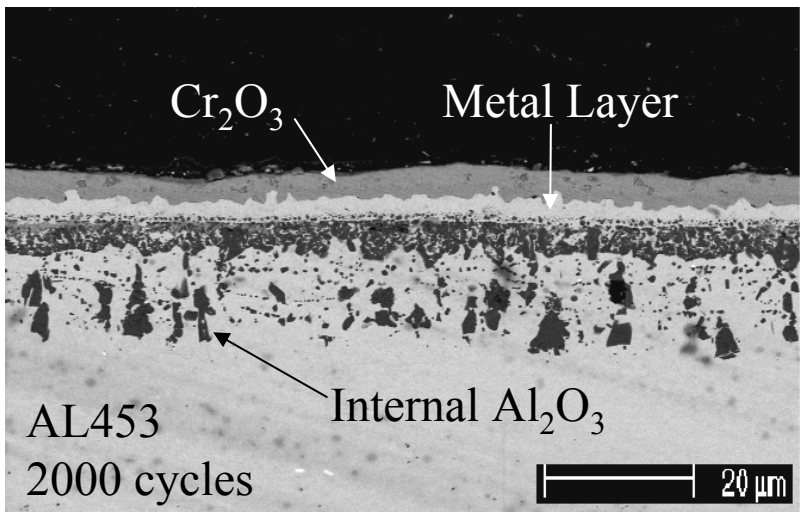

Comparison of Crofer at Different Temperatures and Atmospheres

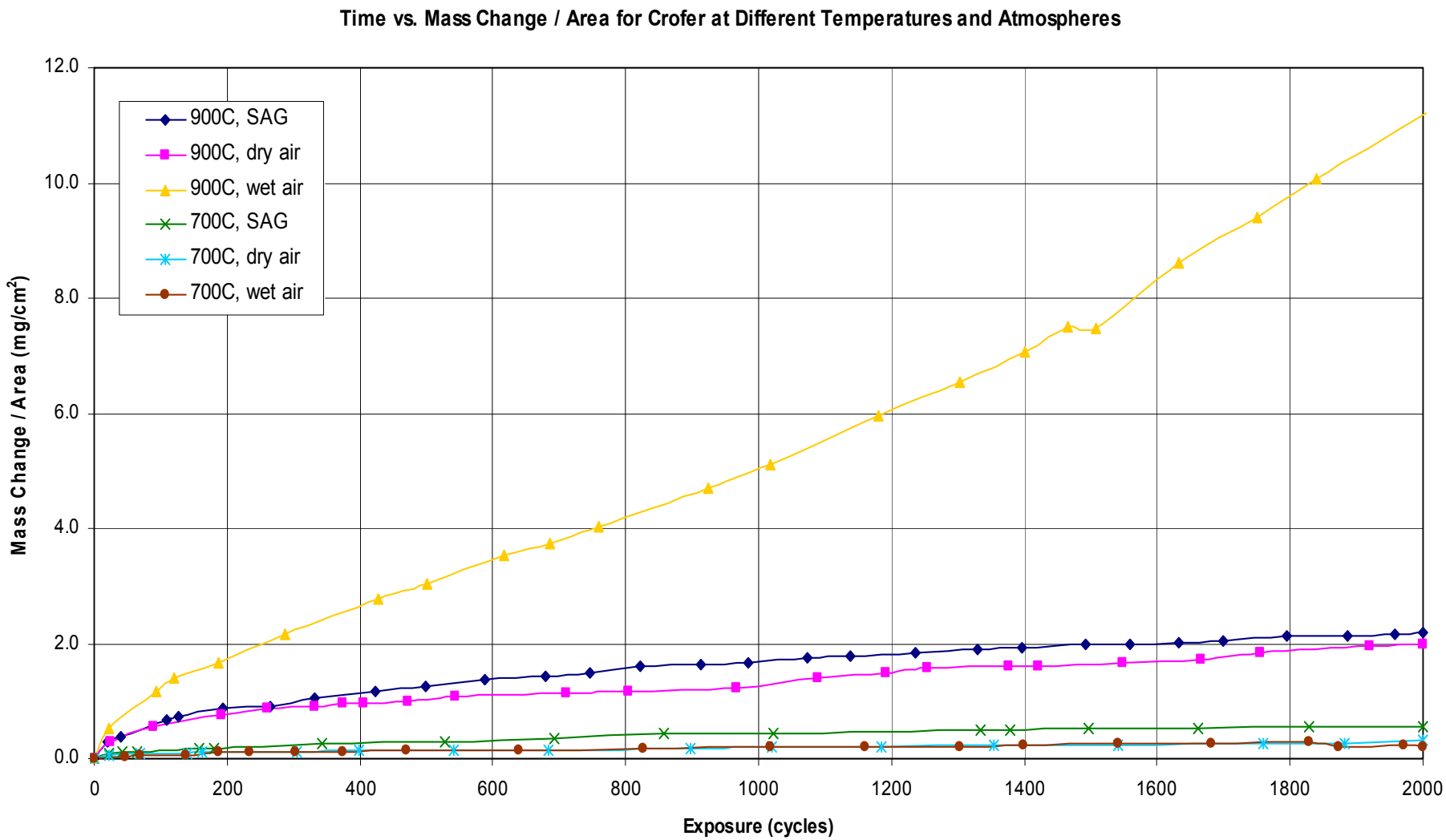

Electrical Conduction of NiO

- E_g=4.2ev, extrinsic behavior
- $Ni_{1-x}O$,$Ni^{2+} \rightarrow Ni^{3+}$ to preserve charge neutrality
- Ni^{3+} provide electron holes, the dominant electrical carrier
- The greater the non-stoichiometry, the greater the conductivity.

Results- Crofer Dry Air Sample

Chromia Layer 1µm thick

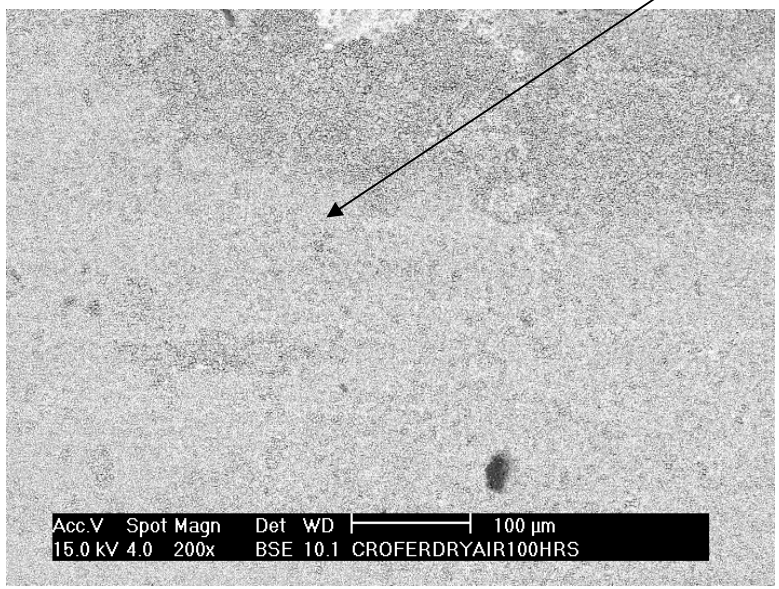

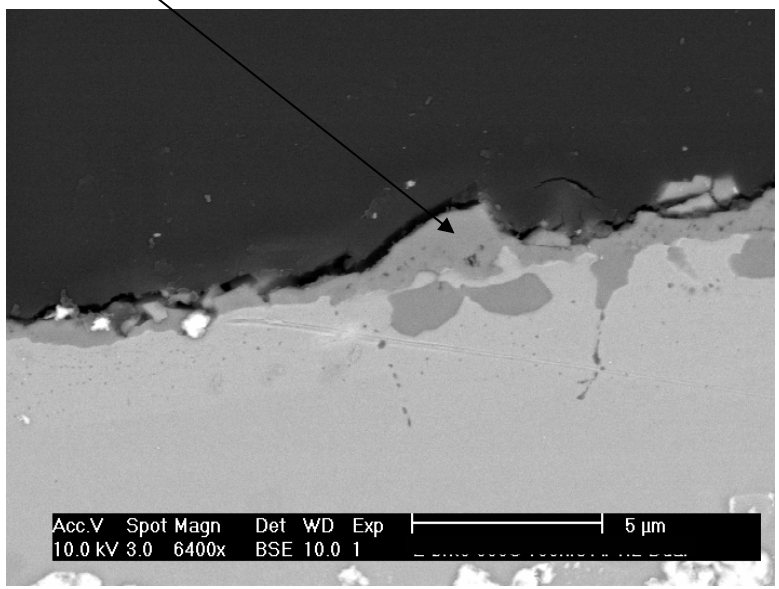

Results-Crofer Dual Atmosphere Apparatus- Air side

Spinel Structure-
$(Cr, Mn)_3 O_4$

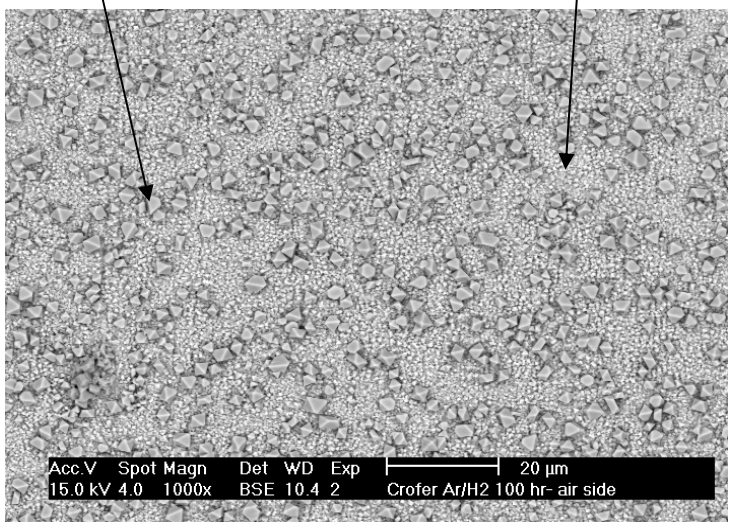

Chromia Layer

Mn

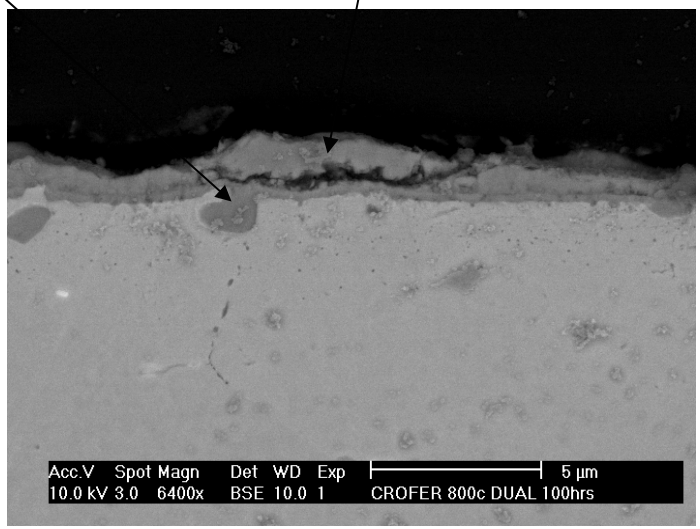

Total oxide thickness was 2µm.

Growth of NiO

- Under strong oxidizing environments NiO exists as a metal deficient oxide
- Ni vacancies are the dominate defect
- The growth of NiO is dominated by the outward transport of Ni through the oxide scale.
- The greater the non-stoichiometry, the faster the growth

Reduction of Growth Rate

- Grain boundary diffusion plays an increasingly important role in oxide growth as the temperature decrease
- Inhibit grain boundary diffusion by the addition of a reactive element
- The growth of NiO has been reduced by an order of magnitude by the coating pre-exposed Ni with Ca, Sr, or other RE
- Pulsed Laser Deposition CeO_2, SrO

Improved Conductivity

- [holes] is fixed by the oxygen partial pressure for pure NiO
- Doping
  - M^{3+} will increase [V_m], decrease[holes]
  - M^{+} ions will reduced [V_m], increase [holes]
- Ni-5wt%Cu alloy

High Conductivity Via

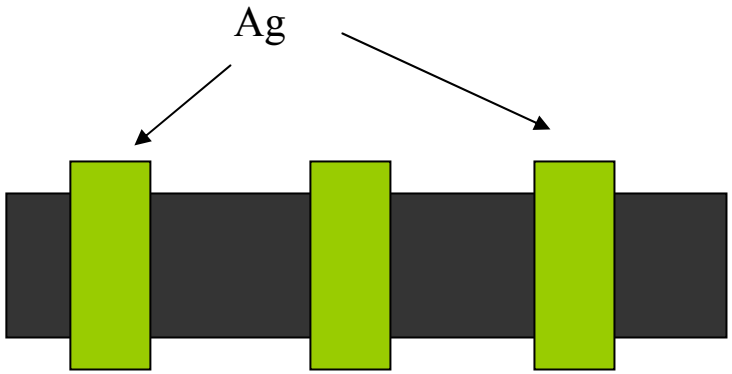

W.A Meulenberg , et al **Journal of Materials Science** 36 (2001) 3189-3195

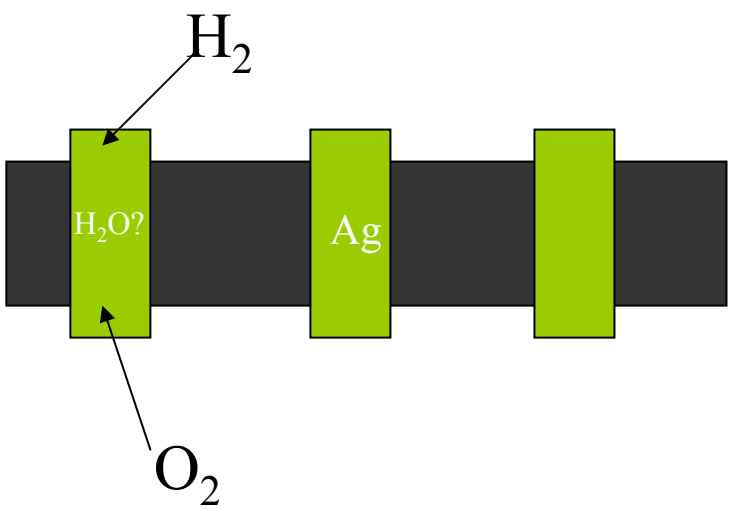

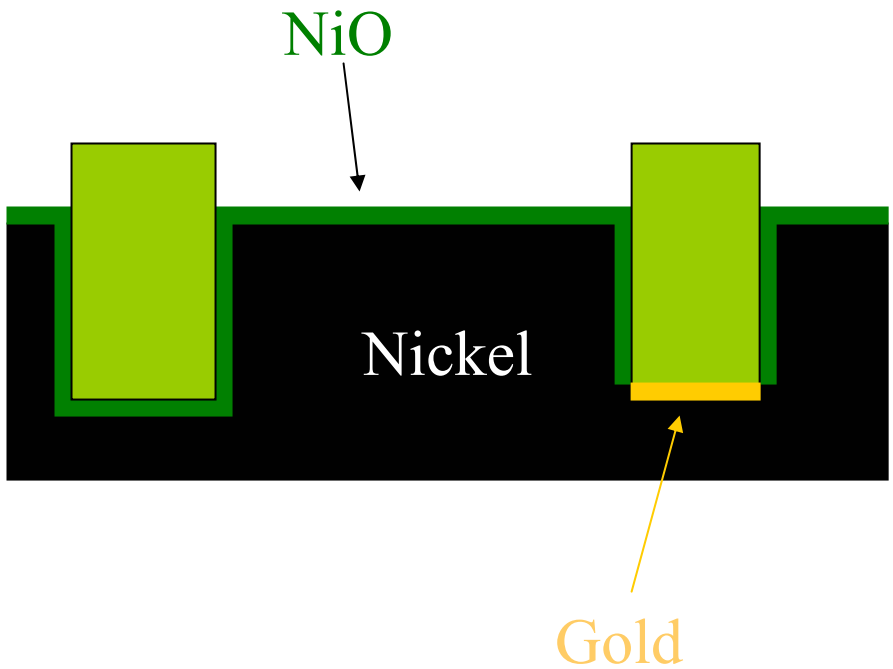

Nickel Mesh

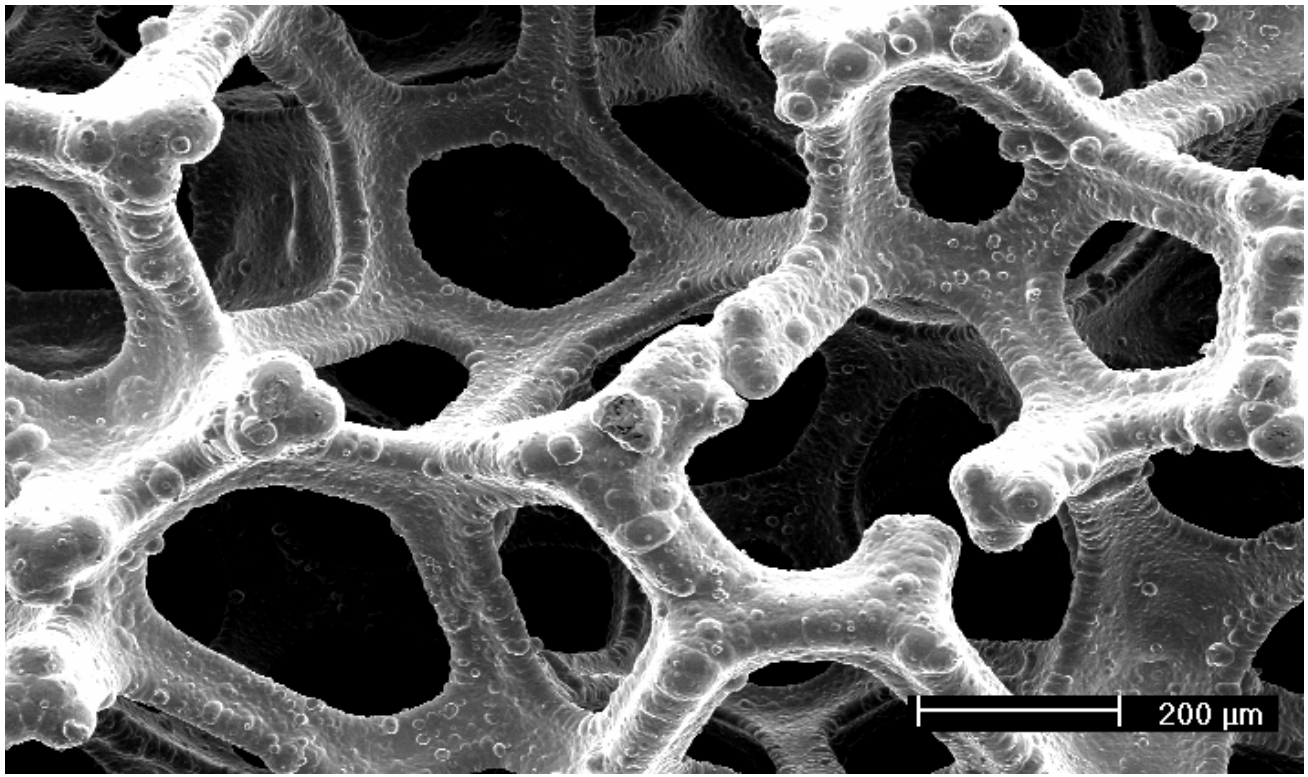

•Fill pores with silver

Pulsed Laser Deposition

- 5 minute deposition time
- 10Hz
- ~10 millijoule
- Total pressure 1.6×10^{-2}torr

SrO Coated Ni